HHS Public Access

Author manuscript

Neuroimage. Author manuscript; available in PMC 2020 January 15.

Published in final edited form as:

Neuroimage. 2019 January 15; 185: 891–905. doi:10.1016/j.neuroimage.2018.03.049.

The UNC/UMN Baby Connectome Project (BCP): An Overview of the Study Design and Protocol Development

Brittany R. Howell[*,1], **Martin A. Styner**[*,2], **Wei Gao**[*,3,4], **Pew-Thian Yap**[*,5], **Li Wang**[*,5], **Kristine Baluyot**[*,5], **Essa Yacoub**[*,6], **Geng Chen**[5], **Taylor Potts**[5], **Andrew Salzwedel**[3], **Gang Li**[5], **John H. Gilmore**[2], **Joseph Piven**[7], **J. Keith Smith**[8], **Dinggang Shen**[5], **Kamil Ugurbil**[6], **Hongtu Zhu**[9], **Weili Lin**[^,5], and **Jed T. Elison**[^,1,10]

[1]Institute of Child Development, University of Minnesota

[2]Department of Psychiatry, University of North Carolina at Chapel Hill

[3]Biomedical Imaging Research Institute, Cedars-Sinai Medical Center

[4]Department of Medicine, University of California, Los Angeles

[5]Biomedical Research Imaging Center, University of North Carolina at Chapel Hill

[6]Center for Magnetic Resonance Research, University of Minnesota

[7]Carolina Institute for Developmental Disabilities, University of North Carolina at Chapel Hill

[8]Department of Radiology, University of North Carolina at Chapel Hill

[9]The University of Texas M.D. Anderson Cancer Center

[10]Department of Pediatrics, University of Minnesota

Abstract

The human brain undergoes extensive and dynamic growth during the first years of life. The UNC/UMN Baby Connectome Project (BCP), one of the Lifespan Connectome Projects funded by NIH, is an ongoing study jointly conducted by investigators at the University of North Carolina at Chapel Hill and the University of Minnesota. The primary objective of the BCP is to characterize brain and behavioral development in typically developing infants across the first 5 years of life. The ultimate goals are to chart emerging patterns of structural and functional connectivity during this period, map brain-behavior associations, and establish a foundation from which to further explore trajectories of health and disease. To accomplish these goals, we are combining state of the art MRI acquisition and analysis techniques, including high-resolution structural MRI (T1- and

Address correspondence to Jed Elison (jtelison@umn.edu) or Weili Lin (weili_lin@med.unc.edu). Corresponding Author: Jed T. Elison, Ph.D., Institute of Child Development, 51 East River Pkwy, Minneapolis, MN 55455, jtelison@umn.edu.

*Equal contribution

^Shared senior authorship

Declaration of Interest

Conflicts of interest: none.

T2-weighted images), diffusion imaging (dMRI), and resting state functional connectivity MRI (rfMRI). While the overall design of the BCP largely is built on the protocol developed by the Lifespan Human Connectome Project (HCP), given the unique age range of the BCP cohort, additional optimization of imaging parameters and consideration of an age appropriate battery of behavioral assessments were needed. Here we provide the overall study protocol, including approaches for subject recruitment, strategies for imaging typically developing children 0 – 5 years of age without sedation, imaging protocol and optimization, a description of the battery of behavioral assessments, and QA/QC procedures. Combining HCP inspired neuroimaging data with well-established behavioral assessments during this time period will yield an invaluable resource for the scientific community.

Keywords

Baby Connectome Project; MRI; dMRI; DTI; rfMRI; neurodevelopment; behavior; infancy; Lifespan Connectome Project

1. Introduction

The Human Connectome Project (HCP) has fundamentally altered MRI-based neuroimaging research (Glasser et al., 2016a; Van Essen et al., 2013; Ugurbil et al., 2013). Indeed, the approach to acquisition and processing, and the quality of HCP and HCP-inspired data has advanced our knowledge of the structural and functional network architecture of the brain (Glasser et al., 2016b; Tavor et al., 2016). These innovations have been incorporated into other major neuroimaging efforts including, but not limited to, The Developing Human Connectome Project (http://www.developingconnectome.org/project/) in the UK, the UK Biobank (http://www.ukbiobank.ac.uk/; Miller et al., 2016), the Adolescent Brain Cognitive Development (ABCD) Study (https://abcdstudy.org/), and the family of Lifespan & Disease Connectome projects funded by the National Institutes of Health in the U.S. Among these studies, the Lifespan Connectome Projects aim to complement the recently completed young adult HCP (25–35 years of age) by acquiring high quality MR images from healthy subjects between 0–5 years of age (Baby Connectome Project (BCP)), 5–21 years of age (HCP Development) and older than 36 years of age (HCP Aging). Together with the HCP, high quality MR images encompassing the entire lifespan will be made available to the scientific community, enabling detailed and comprehensive investigations of brain structural and functional changes throughout the lifespan. Given the ultimate goal of the Lifespan Connectome Projects, experimental protocols, including imaging and cognitive assessments, similar, or better yet identical, to that of the HCP are clearly desirable. Similar to the Development and Aging Lifespan Connectome Projects, which used a modified version of the young adult HCP protocols, the unique age range of the BCP makes it impractical to adopt the original HCP imaging protocol or the behavioral assessment battery. To this end, we describe the rationale motivating the protocol decisions, which are detailed below.

Early brain development, particularly during the first five years of life, can be characterized by dynamic and complex structural and functional development that coincides with remarkable cognitive and behavioral changes. Paralleling the dramatic changes in

morphometric growth rates observed in the latter half of the first year of life, this time period encapsulates the emergence of some of the most important, foundational events in the course of human ontogeny. Joint attention emerges around 9–10 months (Elison et al., 2013; Scaife & Bruner, 1975; Carpenter et al., 1998), which includes a set of complex behaviors considered as necessary precursors for: 1) subsequent social-communication (Bates et al., 1979) such as the acquisition of spoken language, along with 2) more complex social-cognitive capacities (Mundy & Newell, 2007; Tomasello et al., 2005) such as Theory of Mind (Kristen et al., 2011; Nelson, Adamson, & Bakeman, 2008). Working memory capacity rapidly increases during this interval (Pelphrey et al., 2004; Reznick et al., 2004; Short et al., 2013), laying the foundation for the development of more complex executive functioning. Additional precursors to more complex cognitive skills, like inhibiting a pre-potent response and effortful/regulatory control, also emerge during this period (Diamond, 2013). Infants between 9–10 months of age also begin to evidence more specialized face processing skills (e.g., losing the ability to effectively/consistently discriminate faces from other species, Pascalis et al., 2002) and specialized language processing (e.g., losing the ability to discriminate non-native language phonemes, Kuhl et al., 2003). Compelling results also indicate that electrophysiological correlates of perceptual binding (Csibra et al., 2000), and perhaps even perceptual consciousness (Kouider et al., 2013) can be detected during the latter half of the first year of life. The second and third years of life are exemplified by symbolic and conceptual representations culminating in receptive and expressive language skills, as well as continuous refinement of executive functioning skills. The constructive and continuous refinement of cognitive capacities during this age reflects the steady rates of change in morphometric and connectivity metrics.

However, we know surprisingly little about how emerging patterns of structural and functional connectivity support and/or enable complex information processing capacities and conceptual representation during the first several years of life. Infant and toddler neuroimaging has evolved substantially over the past 30 years (Barkovich et al, 1988; Chugani & Phelps, 1986; Chugani et al., 1987; Huppi et al., 1991; Mukherjee et al., 2001; Pfefferbaum et al., 1994) with aspects of the current state of knowledge summarized in several recent review papers (Cao, Huang, & He, 2017; Dehaene-Lambertz & Spelke, 2015; Grayson & Fair, 2017; Gao et al., 2016; Huppi, 2011) and highlighted in the current issue. The field leaped forward with the advent of non-invasive data collection procedures, specifically acquiring data during natural sleep (Courchesne et al., 2000; Huppi et al., 1998; Neil et al., 1998), and the promise of infant/toddler developmental neuroimaging was formalized with the initiation of the NIH MRI Study of Normal Brain Development (https://pediatricmri.nih.gov/nihpd/info/index.html). This study set the bar for large-scale multi-institution efforts focused on infant/toddler brain imaging (Evans AC, 2006; Almli et al., 2007) and continues to yield important findings (e.g., Leppert et al., 2009; Fonov et al., 2011; Hanson et al., 2013).

Complementing the NIH MRI Study of Normal Brain Development, a number of independent research groups have produced important findings regarding structural brain development (Knickmeyer et al., 2008; Gilmore et al., 2012; Holland et al., 2014; Remer et al., 2017; Lyall et al., 2015) and white matter development via diffusion tensor imaging (DTI) across the first few years of life (Ball et al., 2013; Ball et al., 2015; Dubois et al.,

2016; Huang et al., 2015; Lee et al., 2016). A smaller number of more recent studies have also begun elucidating the nature of intrinsic functional connectivity networks across the infant/toddler period (Demaraju et al., 2014; Emerson et al., 2016; Gao et al., 2009; Gao et al., 2015; Graham et al., 2016; Lin et al. 2008, Pruett et al., 2015; Qiu et al., 2015; Smyser et al., 2010; Toulmin et al., 2015). Augmenting the work on typically developing infants is a large corpus of neuroimaging literature on infants born premature (Brown et al., 2009; Cao et al., 2016; Huppi et al., 1991; Huppi et al., 1998; Inder et al., 2005; Kidokoro et al., 2014; van den Heuvel et al., 2014). Lastly, the promise of infant/toddler neuroimaging for informing the subsequent emergence of atypical patterns of behavior is highlighted by recent findings from the Infant Brain Imaging Study or IBIS (http://www.ibis-network.org/) (Emerson et al., 2017; Hazlett et al., 2017; Lewis et al., 2017; Shen et al., 2017; Wolff et al., 2017).

While there are unique challenges to acquiring MRI data from naturally sleeping infants (approaches to mitigate these challenges are detailed below), the infant brain also poses image processing challenges, exemplified by tissue intensity inhomogeneity, which can be exacerbated by suboptimal orientation within the headcoil elements. Improving tissue segmentation algorithms for the infant brain has required extensive effort (Kim et al., 2013; Wang et al., 2015; Zhang et al., 2015; 2016).

While results reported by these previous studies have certainly provided great insights into early brain structural and functional development, they share several common limitations. First, the bulk of infant/toddler neuroimaging studies have employed cross-sectional designs. Informed by work in school-age children (Giedd et al., 1999; Gogtay et al., 2004; Lebel & Beaulieu, 2011; Shaw et al., 2006), longitudinal studies have proven necessary to circumvent common inferential errors made about the shape of developmental change derived from cross-sectional data (Kraemer et al., 2000; Raudenbush, 2001; Willett, Singer, & Martin, 1998). Second, although hybrid cross-sectional and longitudinal designs have been employed by several research groups, the sampling schemes are largely sparse with a long duration between two adjacent time points and there are very few examples in the literature of specific children contributing more than 2–3 imaging data points. The capacity to delineate the presence of nonlinear inflection points of structural and functional developmental trajectories during the first 5 years of life requires dense sampling within individuals, examples of which are beginning to appear (e.g., Gao et al., 2015; Holland et al., 2014). Finally, targeted age appropriate cognitive and behavioral assessments collected concurrently with each imaging visit have been idiosyncratically employed. To mitigate the aforementioned limitations, the primary objectives of the UNC/UMN Baby Connectome Project, a joint effort between investigators at the University of North Carolina – Chapel Hill and the University of Minnesota, are to: 1) collect HCP-inspired neuroimaging data from 500 children across the first 5 years of life (more on the sample and sampling scheme below), 2) complement the high-quality neuroimaging data with the acquisition of phenotypic data that represents critical domains of cognitive, motor, and social-cognitive functioning during this time frame, and 3) share these data with the scientific community (Nichols et al., 2016).

2. Materials and Methods

The BCP leverages two existing NIMH funded studies to supplement the hybrid accelerated longitudinal and cross-sectional study design. Fifty-six cross-sectional data sets from PI J. Gilmore's R01 (HD053000) will be included in the final BCP sample. One hundred individuals from PI J. Elison's R01 (MH104324), 60 longitudinal and 40 cross-sectional, will also be included in the final BCP sample. To maximize our ability to detect inter-individual differences in the presence of intra-individual change over time, the majority of the participants (n = 285) will contribute between 4 and 6 longitudinal imaging & behavioral data points, with the remainder (n = 215) contributing a single cross-sectional time point. See Table 1 for summary of the longitudinal sampling plan. A single cross-sectional scan and behavioral assessment will be collected in 10 children at each of the following ages; 3, 6, 9, 12, 34, 37, 42, 44, 52, 53, 55, and 56 months (n = 120). An additional 25 children will enroll at each 47, 48, and 49 months. Lastly, 20 children will enroll at 60 months, for a grand total of 215 cross-sectional data points.

2.1 Participants

A total sample of 500 typically developing infants, toddlers, and preschool-aged children will be recruited and enrolled between birth and 5 years of age. Participants will be recruited from existing registries at UNC and UMN based on state-wide birth records as well as from broader community resources (e.g., community centers and targeted day-care centers) to ensure the sample approximates the racial/ethnic and socio-economic diversity of the US census. To augment recruitment of the youngest cohort of participants, we may recruit participants perinatally by approaching expectant and new mothers at "The Birthplace" at UMN and the UNC Hospitals Newborn Nursery. Parents of all participants provide permission and informed consent prior to participation. All procedures were approved by the University of North Carolina at Chapel Hill and the University of Minnesota Institutional Review Boards.

Inclusion and Exclusion Criteria—Children are eligible for enrollment into the BCP if they are between the ages of 0–60 months. They are also eligible if they were 1) born at a gestational age of 37–42 weeks, 2) had a birth weight appropriate for gestational age, and 3) had an absence of major pregnancy and delivery complications. Children are excluded from the BCP if they were born prior to 37 weeks gestation, had a birth weight lower than 2,000 grams, or if they had any major delivery complications. Major delivery complications may include neonatal hypoxia or neonatal illness requiring a greater than two day NICU stay. They are also excluded if they: 1) are adopted, 2) have a first degree relative with autism, intellectual disability, schizophrenia, or bipolar disorder, 3) have any significant medical and/or genetic conditions affecting growth, development, or cognition, or 4) have any contraindication to MRI. Additional exclusion criteria include major pre- and/or perinatal issues including: 1) maternal pre-eclampsia, placental abruption, maternal HIV status, and maternal alcohol or illicit drug use during pregnancy. Finally, children are excluded from the study if their caregivers are unable to communicate in English at a level to provide informed consent.

2.2 Subject Flow

Information collected prior to the day of imaging—To confirm study eligibility and gather other necessary information prior to study enrollment, a telephone screening is completed with the child's caregiver. This telephone screening gathers basic family information for the child, parents, and siblings. This information includes date of birth, child's place of birth, race, ethnicity, language(s) spoken in the home, parental education and occupation, household annual gross income, and contact information (address, phone, email). The telephone screening then reviews all exclusionary factors listed above in yes/no format for the caregiver to confirm or deny. Next, medical history related to the child is reviewed that may pertain to MRI, which includes previous medical/surgical problems, hospitalization, previous surgeries, medications, allergies, doctor's visits, and previous MRI experiences. Families are asked for updates on their child's health at each visit to ensure there are no changes in health or continued eligibility. Lastly, information directly related to the likelihood of completing an MRI and/or study visit is obtained. This includes how the child responds to: new experiences/people, being asked to stay in one place, and enclosed areas. We also ask the caregiver to give details regarding when the child is the most calm or soothable, their typical nap/sleep schedule, and their current reading/communication skills.

Once this information is collected and it is confirmed that the child is eligible for the study, the caregiver is contacted to schedule their first BCP visit. This visit is scheduled around a specific age that directly relates to the cohort that they are being enrolled into. For younger children (0–35 months), this visit is scheduled directly around the child's typical nap or sleep time, whichever the caregiver prefers. In addition, it is common to schedule two visits with the scan time varying between one naptime scan and one bedtime scan, to have the most optimal time for the child. Older children (36–60 months) may participate in a scan while sleeping or awake depending on the information provided by the parent. If asleep, these scans are scheduled at nighttime, due to the inconsistency of naps in older children. If awake, there will be two BCP visits scheduled, which will include a training MRI session and the scheduled MRI. See Figure 1 for representation of subject flow.

Training Session—Children scheduled to complete an awake scan are also scheduled to complete a training "mock scanner" session. This session is completed to review all details surrounding the MRI scan to accurately prepare children (and their families) to reduce fear and anxiety that can be associated with new experiences. Before beginning the session, children watch an MRI video that shows another child getting ready for and starting their MRI scan. After watching this video, the children go through the same steps of the MRI as they will for their scheduled scan. First, they practice wearing earplugs and lying down on the scanner bed. Once the child is comfortable, the head coil is placed and they are rolled into the bore. While in the bore, the iPad in the back of the scanner plays a video and MRI sounds, much like the child will experience during their scan. Throughout this practice session, the child is reminded to lay still and watch their video.

Children who become too distressed during the training session (e.g., unable to lay down, go into the bore, etc.) are not forced to practice. It is then decided by the caregiver and coordinator whether the child is able to complete the scheduled MRI scan. Some children

need multiple training sessions to fully habituate to the scanner environment and others may still be unable to get into the scanner or hold still regardless of training sessions.

Day of Imaging—Prior to arriving for the scheduled MRI, caregivers with children that will complete a sleep scan are encouraged to not allow their child to fall asleep prior to arriving for their scanning session. For younger participants (under a year old), parents are not encouraged to change their child's normal routine. Parents of older participants (12–36 months) may be advised to mildly sleep deprive (i.e. awaken an hour early, or skip a nap) their child to increase the chances of successfully falling asleep in the scanning environment. Upon enrollment, parents of participants are provided with headphones and an audio file of scanner sounds to expose their child to for the week prior to coming in for the scanning session.

When the family arrives for their scheduled visit and MRI scan, they are required to complete all enrollment paperwork before any data is collected (informed consent and HIPPA disclosure). For older children that completed the training session, this paperwork is already completed during that visit. Some children (and their parents) will complete the behavioral assessment battery on the same day of the scan; others may choose to have the behavioral assessments and the scanning session scheduled on separate days.

Sleep vs Awake Scanning Preparation—Regardless of the type of scan the child is completing (sleep versus awake), all children are required to remove any metal from their body. Preschool-aged children may change into facility-provided scrubs. For infants, caregivers are provided with an MRI safe blanket to swaddle their child. Children completing a sleep scan use the time in the preparation/staging room to begin calming and preparing themselves to sleep. The staging room has lighting dimmed for sleep scans and normal lighting for awake scans. Caregivers are encouraged to follow typical bedtime routines as much as possible, including diaper changes, feeding, and book reading, etc. Lastly, prior to entering the scanner room, the MRI technologist places earplugs (for child completing sleep scan) in the child's ears and then covers them with tape. Children completing an awake scan use this time to review their movie choices and choose a movie to watch during their scan. The MRI technologist reviews the MRI screening form with the caregiver to ensure it is safe for both the child and caregiver to enter the MRI room.

Imaging Procedures for Sleep Scan—All scanning of children up to 36 months of age will occur during natural sleep, using similar procedures to those previously documented (Dean et al., 2014; Gilmore et al., 2004; Hazlett et al., 2005; Lin et al., 2008). Families with older children (36 – 60 months) may opt to scan their children while awake or during natural sleep. To ensure maximum sound attenuation, sound attenuating foam is used to line the bore of the scanner. Sand bags are placed on the scanner table and on top of the head coil to help attenuate any vibrations during active scanning. A warming beanbag is placed on the scanner table, which warms up the bed prior to the child laying down. The lights in the scanner room are turned off and a curtain is placed over the observation window (outside of the room) to block out light. All sources of light on the scanner itself are covered using blackout curtains to ensure a dim environment. In addition, the lights in the hallway leading to the scanner room are also turned off during the transition of the child from the prep room

into the scanner room. White noise or scanner sounds are played in the background while participants prepare to be scanned (i.e. falling to sleep), depending on caregiver preference.

When we are ready to begin scanning, the caregiver and child are brought into the scanner room. Caregivers are encouraged to get their child to sleep as they would at home. There is a rocking chair provided and caregivers are able to give their child a bottle/nurse in the staging room (or nurse in the scanner room for young infants). We encourage caregivers to attempt rocking the child to sleep in their arms to allow for easier transfers to the scanner table. When this is not possible, we provide an MR safe crib for the child to fall asleep in prior to being moved to the scanner table. The child should already have earplugs, placed by the MRI technologist (in prep room), as well as headphones. However, if this is not possible prior to scan (due to child distress), this will be done once the child is asleep. Once asleep, the caregiver is instructed to knock on the observation window to instruct the coordinator and/or technologist to enter the room. The caregiver is then instructed to gently place the child on an MR safe infant pad on the scanner table. The child's head is positioned in the head coil using foam pieces to provide support and to prevent motion artifact due to motion related to respiration. If a child's head is too large to fit in the head coil with headphones, sound-attenuating foam is used instead. It is important to note that each time a child has to be moved, regardless of whether they showed overt signs of waking, the child is given time to acclimate and continue falling into a deeper sleep. Parents are invited to remain in the scanner room with their child, but are also welcome to wait in the prep room during the scan. A well-trained staff member remains in the room with the child throughout the entire scan and removes them from the scanner immediately if they wake. This staff person positions themselves near the entrance of the bore and places their arm/hand in a manner to reach the abdomen of the child (no parent or staff member lays in the bore with the child).

Imaging Procedures for Awake Scans—Children ages 36 months and older can complete their MRI scan while awake, based on caregiver suggestion and preference. The scanner table is set to a lower height to allow children to climb up independently, if they so choose. The front of the scanner is decorated with paper cutouts (popular movie characters, flowers, etc.) to create a friendlier environment. The child's movie is already displayed on the screen, but is not yet being played. The lights are left on, but may be dimmed to encourage a child to fall asleep or allow the child to better see the lighting of their movie. The MRI technologist places the earplugs and gets the child to lay back onto scanner table. The child is then instructed to move their head up, as much as possible, into the 32 channel Siemens head coil. Headphones are then placed around the child's ears to help protect the child's ears and aid in listening to the movie. The head coil is then placed with the mirror on top, which allows the child to see the screen at the back of the scanner. Depending on the child, a weighted blanket may be placed on the child's legs to help reduce movement during the scan. Once placed in the bore, caregivers can decide to stay in the scanner room or leave. A well-trained staff member remains in the room with the child throughout the entire scan to remind the child to hold as still as possible and removes them from the scanner, if necessary.

2.3 MRI Imaging Protocols

Images are acquired on 3T Siemens Prisma MRI scanners using a Siemens 32 channel head coil at the Center for Magnetic Resonance Research (CMRR) at the University of Minnesota and the Biomedical Research Imaging Center (BRIC) at the University of North Carolina at Chapel Hill. Built on the imaging protocol developed by the Human Connectome Project (Van Essen et al., 2013) and the current Lifespan HCP, the BCP imaging protocol consists of four main sequences, T1w, T2w, resting-state functional connectivity (rfMRI – exactly as collected in the Lifespan HCP), and dMRI, respectively. The first sequence collected is a localizer sequence modified to be quieter than typical localizers by lengthening the TR from 8 msec to 30 msec, and the TE from 4 to 5 msec to minimize waking in participants scanned during sleep (see Table 2 for imaging sequence protocols). T1- and T2-weighted images are acquired to provide information regarding structural brain development. A 3D variable flip angle turbo spin-echo sequence (Siemens-Space) was used for T2 weighted images (turbo factor=314, echo train length of 1166 msec) (Mugler et al., 2000). T1- and T2-weighted images were prioritized first, followed by resting state rfMRI and diffusion imaging (dMRI). Both rfMRI and dMRI are collected using single-shot EPI sequences. Prescan normalize is enabled for the T1 and T2 scans, however, unfiltered images are also acquired. No other filters are applied. If data were not of high enough quality for analysis (i.e. considerable motion was observed at the time of scanning), they are reacquired if possible. The rfMRI, T1w, and T2w imaging parameters largely match the other Lifespan HCP projects in spatial and temporal resolution. However, modification of the diffusion protocol was necessary to optimize acquisition parameters for characterization of both fiber orientation estimation and microstructure for the age range of this study. Specifically, we piloted three different diffusion protocols for further evaluation (the results of which are provided in section 2.5).

2.4 Quality Assurance/Assessment and Minimal Processing

Radiological Review—The anatomic images from each subject's MRI are transferred to a DICOM workstation (Osirix, Pixmeo SARL, 266 Rue de Bernex, CH-1233 Bernex, Switzerland) for review. A board certified neuroradiologist (JKS) reviews the images for any clinically or research relevant incidental findings. Review results are recorded using a Qualtrics (333 W River Park Dr, Provo, Utah) database web case report form. Any clinically relevant findings are also reported directly to the PIs to relay to the participant’s caregiver. The neuroradiologist facilitates any needed clinical evaluation or follow up with phone consultation with the participant’s caregiver or their medical provider, if needed. Reviews typically occur within 2 weeks of data acquisition.

Structural MRI (sMRI)—Incoming structural MRI data are assessed visually for excessive motion, insufficient coverage, and/or ghosting. Visual motion assessment is performed on a four-point scale (reject, major motion/borderline, minor motion/pass, excellent). Borderline scores are given to scans with an intermediate potential of processing failures. If multiple scans were made acquiring a structural MRI modality, and all individual scans are rated fail or borderline, we attempt to rescue the scans via co-registration and weighted averaging with weights depending on the visual rating of the scan quality. Data is then rigidly aligned into ICBM space via a 1–2 year old pediatric template (Hazlett et al., 2017), followed by N4 based intensity inhomogeneity correction (Tustison et al., 2010). All datasets were registered

into the 1–2 year old pediatric atlas space, whether they were younger than 1 year or older than 2 years. While infant templates are available (and our group is actively disseminating such templates), there is no significant difference in *rigid* alignment when a 1–2 year template is employed rather than a neonate infant template. This was done as to not introduce an age-dependent bias this early in the processing. Thus we used the single template that is most appropriate for the full age range in the study (0–5 years). Brain masks are determined via a multi-atlas based skull stripping (Wang et al., 14), followed by manual correction. Further processing and registrations will be completed using the multiple age-specific templates our team has developed that include the first two years of life, including infant, 3, 6, 9, 12, and 24 months old templates from an earlier study where subjects were longitudinally imaged at 2–4 wks, 3mons, 6mons, 9mons, 12mons, 18mons and 24mons (PI: Lin).

Diffusion MRI (dMRI)—Diffusion data suffers from inherently low SNR, motion, eddy current, and susceptibility artifacts. Thus, all our datasets are subjected to strict and thorough quality control procedures. Our diffusion data is collected in pairs with reverse phase-encoding blips, which results in susceptibility-induced geometric distortions in opposite directions. These distortions are corrected by first applying the TOPUP tool (Andersson et al., 2003) from the FMRIB Software Library (FSL) (Jenkinson et al., 2012), which results in a single corrected image. We chose to collect reverse phase encoding directions for EPI sequences despite the increased acquisition time so as to maintain compatibility with the other Lifespan HCP protocols. Additionally, accurate spatial matching between anatomical and diffusion images is important, for example, for cortico-cortical connectivity analysis. Then, DTIPrep (Oguz et al., 2014) is employed to identify and exclude dMRI volumes with corrupting artifacts, as well as to apply corrections for motion and eddy current artifacts. The detected motion is quantified and recorded for use in the analysis, for example to co-vary for motion related effects. Datasets with more than 20% rejected dMRI volumes were judged to fail QC. At present, while most acquired dMRI scans had a least one rejected dMRI volume, 89.54% of the acquired diffusion scans passed QC. Due to the relatively large FOV used to ensure consistency across the large age range, 15% of the dorsal slices and 20% of ventral slices were skipped during DTIPrep QC for infants 6 months-old and younger. Next, diffusion MR models are estimated for tensor data (weighted least square), NODDI data (neurite orientation dispersion and density imaging: Zhang et al., 2012), and fODF (fiber orientation distribution function). Visual inspection of the local major orientation and all modeled diffusion data is performed, as well as fiducial probing based tractography of the tensor data to establish appropriate tracking of the major fiber tracts (e.g., genu, splenium, tapetum, cingulate, uncinate, cortico-spinal tract, fornix, inferior longitudinal fasciculus, etc.).

Resting state functional connectivity MRI (rfMRI)—We also measure resting state based brain connectivity via fMRI. Such rfMRI data relies on accurate quantification of the temporal correlation between distant voxels in the brain. As for other MRI data, subject motion is known to potentially contaminate the rsfMRI signal, thus additional steps are required to insure proper QC for infant rsfMRI imaging (Gao et al, 2015). Thus to identify scans where motion may potentially lead to problems during processing we are using the

FIRMM (framewise integrated real-time MRI monitoring) software package during rfMRI acquisition (Dosenbach et al., 2017). Functional data is corrected for spatial distortions due to gradient nonlinearity, B0 inhomogeneity, and head-motion. Frame censoring or "scrubbing" (which used to be optional in the HCP pipeline) is mandated in order to further control for more frequent motion related artifacts in naturally sleeping infants. Thresholds for the censoring step are based on frame-to-frame changes in spatial displacements (>0.5mm) (Power et al, 2012) as measured via FSL's fsl_motion_outliers. Minimally 50% of the acquired volumes (210 of 420 planned volumes) must show a frame-wise displacement below the threshold in order for the scan to pass QC. We acquire both AP and PA sensitized rfMRI data. QC and connectivity processing are applied separately and the resulting connectivity matrices are fused as a final step of the processing.

2.5 Diffusion MRI Optimization and Results

It has been widely demonstrated that water mobility is greater in infants as compared to adults, reflecting, potentially, less biological barriers than the adult brain. In addition, unlike adult studies, where a long acquisition time can be used for dMRI, the acquisition time available for imaging non-sedated typically developing children is limited. Together, a modification of the HCP/Lifespan HCP dMRI protocol, including gradient sampling schemes, b-values, and number of shells, which was optimized for adults, warranted modification for our cohort. To this end, three sampling schemes were evaluated: Modified versions of 1) the HCP Development (DHCP) and 2) the HCP Lifespan Pilot Project (LHCP) sampling schemes and 3) a 6-shell sampling scheme. The main objective was to determine which approach provides the lowest errors for estimating fractional anisotropy, mean diffusivity, principle tensor direction and orientation distribution function to identify the dMRI protocol that provides suitable tensor estimation while also providing flexibility for various modeling techniques across this unique age range.

For all sampling schemes, diffusion-weighted (DW) images were collected at UNC and UMN sites from a total of 10 pediatric subjects – two at each of 5 time points: 0.5 months, 3 months, 6 months, 12 months, and 24 months. All data were collected with 1.5mm isotropic resolution, multi-band of factor 5, and phase encoding in the anterior-posterior direction. The sampling schemes only differed in the diffusion weightings (i.e., *b*-values) and diffusion-sensitizing, non-collinear gradient directions (see Table 3 and Figure 2 for example data).

For each subject, the reference dataset used for evaluation was formed by combining the datasets from the three sampling schemes, resulting in a total of 454 images (428 diffusion-weighted images and 26 non-diffusion-weighted images). The images were corrected for eddy-current and motion artifacts before they were used for evaluation (Andersson et al., 2016; Andersson & Sotiropoulos, 2016). All diffusion-weighted images were used to fit the tensor model as previous work has shown that inclusion of high b-value images can improve tensor calculation (Veraart et al., 2011).

We first computed the normalized absolute difference (NAD) between the fractional anisotropy (FA) and mean diffusivity (MD) values given by each sampling scheme and the reference. Normalization was performed with respect to the reference value. Figure 3 shows

the absolute difference in FA and MD as compared to the reference dataset for each sampling scheme in a dataset from a 6-month-old. Figures 4 and 5 show the voxel-averaged NAD values of FA and MD, respectively, indicating that the 6-shell sampling scheme results in the least errors.

We use orientational discrepancy (OD) (Yap et al., 2011) for quantitative evaluation of the estimated fiber orientations using the diffusion tensor (DT) model and a multi-tissue (MT) model presented in (Yap et al., 2016). Smaller OD values indicate greater accuracy. For the DT model, the fiber orientation was given by the tensor principal direction. For the MT model, fiber orientations were detected from the fiber orientation distribution function (ODF) using the method presented in Yap and Shen, 2012. Figure 6 shows the OD values for the DT model in the white matter. Figure 7 shows the OD values for the centrum semiovale, which contains three-way fiber crossings (Fernandez-Miranda et al., 2012). These results indicate that the 6-shell sampling scheme allows local fiber orientations to be estimated with increased accuracy.

As such, all new enrollees in the BCP will be scanned with the 6-shell sequence described above. If the participants continue to sleep beyond the second set of resting BOLD sequences, we will attempt a 2-shell version of the HCP Lifespan Pilot Project (79 directions, b-values of 1500 and 3000, MB=4) as a substantial portion of data has already been collected with this sequence as part of J. Elison's R01 (which began in 2014). We will prioritize the 79 direction 2-shell sequence for those children who are completing longitudinal visits as part of that project to maintain longitudinal compatibility, but we will attempt the 6-shell version for those children who sleep beyond the second set of resting BOLD sequences. This scenario applies to participants in cohorts E1-E4 in Table 1.

2.6 Behavioral Procedures

A battery of age appropriate behavioral assessments and parent report questionnaires and interviews were selected to provide a targeted characterization of developmental functioning. The behavioral battery was designed with 3 constraints/opportunities in mind. 1) Very few NIH toolbox measures are validated for children under the age of 5, therefore diminishing the possibility of implementing the same behavioral assessments & procedures as the Developing & Aging Connectome projects. 2) Very few constructs can be examined meaningfully across the entire 5-year range (e.g., executive functioning), therefore we include repeated assessments of salient constructs within age-appropriate windows of time. 3) We selected constructs and instruments that characterize meaningful variability across the typical-to-atypical continuum, operating under the assumption that this cohort of individuals could be leveraged as a comparison sample for investigations of children at risk for various forms of early emerging emotional, behavioral, and neurodevelopmental disorders. Lastly, we constructed the behavioral battery while considering the promise of new approaches for characterizing associations between select behavioral/cognitive constructs and whole-brain patterns of connectivity (Eggebrecht et al., 2017; Marrus et al., 2017).

2.6.1 Direct Assessment of NIH Toolbox Compatible Constructs—The Mullen Scales of Early Learning (MSEL; Mullen, 1995) provides a standardized assessment of

language, motor, and perceptual abilities for children of all ability levels through 5 years of age. The revised and updated version yields age-normed t scores, age equivalent scores, and percentile rankings for 5 subdomains: 1) gross motor, 2) fine motor, 3) visual reception, 4) receptive language, and 5) expressive language. Scores from the fine motor, visual reception, receptive language, and expressive language domains can be aggregated to yield an Early Learning Composite or developmental quotient value. It is also common to derive verbal (receptive language age equivalent score + expressive language age equivalent score/ chronological age *100) and nonverbal (fine motor age equivalent score + visual reception age equivalent score/chronological age *100) developmental quotient scores from this assessment. The assessment takes between 20–45 minutes, depending on the age of the child. We will implement the MSEL at every behavioral visit between 3 and 60 months of age.

The Minnesota Executive Function Scale (MEFS; Carlson & Zelazo, 2014) is a direct, nationally normed assessment of cognitive flexibility in children as young as 2 years of age administered on an iPad. This age-appropriate virtual card-sorting task has been used with over 20,000 children, an original variant of which has shown excellent test-retest reliability (Beck et al., 2011). Past studies have established multiple forms of criterion validity for the MEFS (Doom et al., 2014; Fuglestad et al., 2015; Hassinger-Das et al., 2014; Prager, Sera, & Carlson, 2016). The MEFS takes approximately 5 minutes to complete and is collected at every behavioral visit between 24 and 60 months of age.

2.6.2 Additional Direct Assessments—The Dimensional Joint Attention Assessment (DJAA; Elison et al., 2013) was developed by study Co-PI J. Elison. The primary objective of the procedure is to characterize a dimensional rating of responding to joint attention (RJA) that reflects individual differences in RJA performance. Characterizing individual differences in RJA performance is more suitable for brain-behavioral investigations than ordinal ratings of competence. The context of the assessment is designed to elicit naturalistic play-based social interaction between the infant and the examiner. The DJAA will be administered at every behavioral visit between 8 and 15 months of age. The assessment takes approximately 10 minutes to complete.

A 10-minute semi-structured parent-child-interaction will be video recorded and archived. The procedure is semi-structured as we provide a standard set of age appropriate toys/ activities, that vary per age group, otherwise we ask the parent to interact/play with their child as they would normally. Video data will be archived and made available for the scientific community. Various constructs could be extracted from this assessment (e.g., maternal sensitivity, infant social referencing, dyadic contingent responses, etc.) with formal/established (Wan et al., 2017) informal/discovery coding schemes. This procedure is included in each visit between 6 and 15 months of age.

2.6.3 Parent Interviews—The Vineland Adaptive Behavior Scales (VABS II; Carter et al., 1998; Chatham et al., 2017; Sparrow, Cicchetti, & Balla, 2005) assesses child adaptive behavior in communication, socialization, daily living skills, and motor domains. The first edition of this scale had excellent reliability and validity and was sensitive to the gradient of severity of autism spectrum disorder symptomatology. The instrument has proven useful in

differentiating high-risk infants subsequently diagnosed with autism as early as 12 months of age (Estes et al., 2015). The VABS II is implemented at each visit between 3 and 60 months of age. The instrument takes between 15–30 minutes to complete.

The Family Interview for Genetics Studies (FIGS) is designed to characterize family history of mental illness in 1st degree relatives of the child. Administration of the interview proceeds in three steps: 1) a pedigree is drawn and reviewed with the informant, 2) general screening questions are asked in references to all known 1st degree relatives of the child of interest, and 3) based on the informant's responses to the general screening questions, a Face Sheet and one or more symptom checklists (depression, mania, psychosis, alcohol and other drug abuse, ADHD, autism, and obsessive compulsive disorder) are completed for each relative. This interview was also included in the NIH MRI Study of Normal Brain Development. It takes approximately 30 minutes to complete and is conducted over the phone prior to the first visit.

2.6.4 Parent-Report Questionnaires – General—The MacArthur-Bates Communicative Development Inventories (MCDI: Fenson et al., 2007) is a widely-used, norm-referenced parent-report questionnaire designed to index expressive language, language comprehension, and communicative gesture use. We will use the MCDI-Words & Gestures Form between 12 and 24 months and the MCDI-Words & Sentences Form between 25 and 32 months of age. The Words and Gestures Form is normed for use between 8–18 months for typically developing samples. However, based on: 1) our experience with at-risk samples (Swanson et al., 2017) and 2) the likelihood that BCP data may be used as a comparison for at-risk samples, we decided to extend the use of the Words & Gestures Form to 24 months. The forms take approximately 20 minutes to complete. The MCDI will be completed at all visits, yielding between 2 – 5 longitudinal assessments depending on the cohort.

The Infant Behavior Questionnaire-Revised (IBQ-R; Gartstein & Rothbart, 2003) and the Early Childhood Behavior Questionnaire (ECBQ; Putnam, Gartstein, & Rothbart, 2006) are parent-report questionnaires designed to capture profiles of temperament in early childhood. The IBQ-R includes 191 items (comprising 14 subscales) and is used between 3–13 months of age in the current study (captured on 2 occasions). The ECBQ includes 201 items (comprising 18 subscales, 11 of which cross over with the IBQ-R) and is implemented between 21–35 months of age in the current study. The expectation is that dimensions of temperament are rather stable; nonetheless, we collect data on these instruments on two occasions in all longitudinal cohorts. Cohort A will receive the IBQ-R on 2 occasions in the first year of life and the ECBQ at 24 months. All 285 children in the longitudinal cohorts will receive the ECBQ between 21–26 months of age. The instruments take approximately 20 minutes to complete.

The Children's Social Understanding Scale (CSUS; Tahiroglu et al., 2014) is a 42-item parent-report questionnaire that assesses mental state understanding in preschool-aged children. The measure has proven reliable and valid in assessing various categories of early emerging Theory of Mind including *beliefs* about other people (e.g., understands that telling lies can mislead other people), *knowledge* about other people (e.g., realizes that experts are

more knowledgeable than others in their specialty), other person *perception* (e.g., talks about what other people hear or see), *desire* (e.g., talks about the difference between what people want and what they actually get), *intention* (e.g., understands the difference between doing something intentionally and doing it by mistake), and *emotion* (e.g., realizes that if s/he does something bad, others may get mad). The CSUS will be administered to all children at all visits between 24 – 60 months. The instrument takes approximately 10–15 minutes to complete.

2.6.5 Parent-Report Questionnaires – Clinical Dimensions—The Infant Toddler Social Emotional Assessment (ITSEA; Carter et al., 2003) is a 166-item well-established parent-report measure of social-emotional and behavioral development designed to identify early deficits or delays. The ITSEA assesses four domains of functioning that include externalizing behaviors (e.g., impulsivity, aggression), internalizing behaviors (e.g., withdrawal, general anxiety, inhibition to novelty), dysregulation (e.g., negative emotionality, sleep/eating dysregulation, sensory sensitivity), and social competencies. The assessment also captures low base-rate, clinically relevant social behaviors that include maladaptive and atypical behaviors, and unusual patterns of social relatedness. Parents will complete the ITSEA on two occasions, between 12 and 30 months. The instrument takes approximately 15–20 minutes to complete.

The Preschool-Aged Child Behavior Checklist (P-CBCL; Achenbach et al., 2000) is a 99-item, widely-used, norm-referenced, parent-report questionnaire that evaluates a range of internalizing and externalizing symptoms based on six subscales (emotionally reactive, attention problems, anxious/depressed, somatic complaints, withdrawn, and aggressive behavior). Scale and subscale scores are summed and converted to t-scores. The CBCL has strong test-retest and inter-rater reliability for all scales and subscales and is appropriate for children between the ages of 18 and 60 months of age. This instrument will be administered on two occasions for all longitudinal cohorts between 18 and 44 months and will be administered to all cross-sectional enrollees between 18 and 60 months.

The Preschool-Aged Strengths and Difficulties Questionnaire (P-SDQ; Croft et al., 2015) is a 25-item parent-report screener for early emerging forms of emotional and behavioral risk. The items represent potential patterns of risk behavior across 3 primary domains including internalizing problems (e.g, emotional domain), externalizing problems (e.g., hyperactivity and conduct problems), and prosocial behaviors. The P-SDQ will be administered at all visits between 24 and 60 months.

The Video-Referenced Rating of Reciprocal Social Behavior (vr-RSB; Marrus et al., 2015) is a downward extension of the 63-item Social Responsiveness Scale (SRS; Constantino et al., 2003; Constantino & Todd, 2003), which is among the most widely used informant-report instruments in the autism field. Notably, the SRS quantifies trait-like behavior that differentiates autism from control participants, but also differentiates adolescents with a psychotic disorder, adolescents at clinical high risk for a psychotic disorder, and children with disruptive behavior disorders from controls (Cholemkery et al., 2014; Jalbrzikowski et al., 2013). The vr-RSB's use of a video-based exemplar affords increased standardization via direct comparison with the child of interest. A total summary score (48 items) is used to

describe toddlers' reciprocal social communication abilities, with higher scores indicating greater impairment in social communication. This procedure will be implemented at each visit between 16–32 months of age. Children aged 33 months and beyond will receive the preschool version of the SRS (Pine et al., 2006).

3. Results and Discussion

Although the BCP was officially launched in September of 2016, substantial progress has been made in the past year or so. As of February 2018 we've had 564 imaging sessions, and have acquired 413 datasets with T1 and T2 (73%), 342 datasets with T1, T2, and rfMRI (61%), and 240 datasets with T1, T2, rfMRI and DWI (43%). Of participants 36 months or older 1 of 2 (50%) at UMN, and 34 of 34 (100%) at UNC were scanned while awake. Having described the quality of diffusion data above, illustrations of the sMRI and rfMRI data quality are provided below.

3.1 sMRI

An isotropic resolution of 0.8 mm ($0.5mm^3$) is achieved for both the T1w and T2w sequences. For rfMRI an isotropic resolution of 2.0 mm ($8\ mm^3$) is achieved and for diffusion MRI, due to the superb gradient capabilities of the Siemens Prisma, a 1.5 mm ($3.375mm^3$) isotropic resolution could be achieved. Figure 8 shows a comparison from two 2-year-old subjects; one was enrolled in an earlier study (from W. Lin, upper panel) while the other subject is enrolled in the BCP (lower panel). Notice the improved spatial resolution leads to better delineation of different brain structures.

Considering the smaller brain size of our cohort, the improved spatial resolution could have profound implications on the accuracy of tissue segmentation. Figure 9 shows the effects of spatial resolution on tissue segmentation. The images acquired from a BCP subject 18 days of age were down-sampled from the acquired 0.8 mm isotropic ($0.5mm^3$) to 1 mm isotropic ($1mm^3$). We applied a state-of-the-art segmentation algorithm (Wang et al., 2015) to segment the brain images into WM, GM and CSF of both datasets. It is immediately evident that images with 0.8mm ($0.5mm^3$) isotropic resolution result in more detailed gray matter structures. We further compared the WM/GM rendering results with the zoomed views, which also demonstrate the advantage of high resolution in characterizing the detailed structural architecture of the infant brain.

3.2 rfMRI

In addition to improved segmentation accuracy, the improved spatial resolution should enable better functional localization. Subjects (N = 3 females, 3–5 months of age) were retrospectively identified for functional connectivity analyses. Data were processed using FSL (Jenkinson et al., 2012; Smith et al., 2004) and AFNI (Cox, 1996). Image processing was primarily based off the Human Connectome Project (HCP) pipeline (https://github.com/Washington-University/Pipelines). First, duplicate anatomical (T1-weighted) images were aligned and averaged. The averaged anatomical scan was then skull-stripped and segmented into WM, CSF, and GM images. The restored (i.e. bias field corrected) anatomical image

was then aligned to a template (i.e. standard space, UNC 1-YR Template; Shi et al., 2011) using a combined linear plus non-linear approach.

Each functional run (n = 4 per subject; two repetitions with phase encoding in either the AP or PA directions) was corrected for head motion using the single band reference images as the target image, distortion corrected using the spin-echo field map data, and finally registered to the anatomical image using the combined anatomical-to-template linear plus nonlinear warp fields. Functional data were also temporally and spatially filtered using recently defined strategies (Power et al., 2012). Briefly, images with frame-wise displace (FD) greater than 0.2 mm were excised and replaced with surrogate data via linear interpolation. The use of linear interpolation (or other data replacement strategies) reduces anomalous time-series that can arise during the bandpass filtering process. Moreover, segments of data corresponding to less than five consecutive frames with FD < 0.2 mm were also treated in this way. The resulting datasets were then bandpass filtered (0.01–0.08 Hz) and regressed of nuisance signals corresponding to motion, cerebral spinal fluid (CSF), white matter (WM), and grey matter (GM). Derivative and quadratic terms were included in the model resulting in 36 total parameters of no-interest (bandpass filtered at 0.01–0.08 Hz). Note “scrubbed” volumes were censored during the regression step so as not to influence the fitting procedure. Finally, the functional data were concatenated and smoothed (FWHM = 4.0 mm) resulting in a singled smoothed 3D+time dataset for each subject that then underwent preliminary functional connectivity (FC) analyses.

These subjects had ample functional data after the conservative scrubbing approach outlined above (> 600 TRs post-scrubbing). Briefly, seed-based connectivity measures were computed using the automated-anatomical-label (AAL) atlas. Mean whole-brain connectivity maps (Z-correlation > 0.33) were then generated for the left/right pre- and post-central gyrus (Pre/PosCG)—see Figure 10. Several features are worth noting. Specifically, there was abundant bilateral connectivity highlighted by discrete foci and patterning that resembled cortical curvature and folding, likely reflecting the high spatial resolution (2.0 mm^3) of the BCP functional data. More importantly, the improved spatial resolution allows separate evaluation of motor and sensory networks in infants (composite maps), which would not have been possible using a resolution of 4 mm^3.

4. Conclusion

The high-quality neuroimaging data collected as part of the BCP and the dense longitudinal sampling is unprecedented for a cohort in this age range. By combining these data with the wide breadth of behavioral measures and genetic information we will be in a unique position to investigate how emerging patterns of structural and functional connectivity, along with genetics, contribute to individual-based variability in key aspects of behavioral development. This project provides insight into developmental trajectories that may contribute to or signal incipient markers of risk for early emerging neurodevelopmental disorders. Despite the noted advances in infant/toddler neuroimaging over the past 10–15 years, there remains much to be learned regarding the structural and functional network architecture and dynamic patterns of brain-behavior associations across the first years of life. This time of dramatic change represents both a period of pronounced vulnerability to adverse environmental

factors, as well as a window of opportunity for adaptation. We are eager to finalize the pipeline for data sharing and anticipate that the data will be available to the scientific community as early as spring 2019. Data acquired as part of the BCP, and shared with the scientific community, promises to inform novel questions about this complex period of ontogeny.

Acknowledgments

We want to thank the members of the ELAB at the University of Minnesota who contribute to the BCP including Angela Fenoglio, Colleen Doyle, Elizabeth Sharer, Robin Sifre, Carolyn Lasch, Ella Coben, Sooyeon Sung, Kristen Gault, Rachel Roisum, Patrick Johnson, and Laura Thomas; Soma Prum, Amber Leinwand, and Jordan Jimenez at the University of North Carolina at Chapel Hill; and we're indebted to the families who so generously contribute to our research.

Funding

This work described herein is supported by NIH grant (1U01MH110274) and the efforts of the UNC/UMN Baby Connectome Project Consortium, a K award (K01MH109773) to L. Wang, and an NIMH Biobehavioral Research Award for Innovative New Scientists (BRAINS) award (R01MH104324) to J. Elison.

References

Achenbach TM, Rescorla LA. Manual for the ASEBA preschool forms and profiles. Burlington: University of Vermont Research Center for Children, Youth, & Families; 2000.

Almli CR, Rivkin MJ, McKinstry RC. Brain Development Cooperative Group. The NIH MRI study of normal brain development (objective-2): newborns, infants, toddlers, and preschoolers. Neuroimage. 2007; 35:308–325. [PubMed: 17239623]

Andersson JL, Graham MS, Zsoldos E, Sotiropoulos SN. Incorporating outlier detection and replacement into a non-parametic framework for movement and distortion correction of diffusion MR images. Neuroimage. 2016; 141:556–572. [PubMed: 27393418]

Andersson JL, Skare S, Ashburner J. How to correct susceptibility distortions in spin-echo echo-planar images: applicaitn to diffusion tensor imaging. Neuroimage. 2003; 20:870–888. [PubMed: 14568458]

Andersson JL, Sotiropoulos SN. An integrated approach to correction for off-resonance effects and subject movement in diffusion MR imaging. Neuroimage. 2016; 125:1063–1078. [PubMed: 26481672]

Ball G, Pazderova L, Chew A, Tusor N, Merchant N, Arichi T, Counsell SJ. Thalamocortical connectivity predicts cognition in children born preterm. Cerebral Cortex. 2015; 25:4310–4318. [PubMed: 25596587]

Ball G, Srinivasan L, Aljabar P, Counsell SJ, Durighel G, Hajnal JV, Edwards AD. Development of coritical microstructure in the preterm human brain. Proceedings of the National Academy of Sciences. 2013; 110:9541–9546.

Barkovich AJ, Kjos BO, Jackson DE, Norman D. Normal maturation of the neonatal and infant brain: MR imaging at 1.5T. Radiology. 1988; 166:173–180. [PubMed: 3336675]

Bates E, Benigni L, Bretherton I, Camaioni L, Volterra V. The emergence of symbols: Cognition and communication in infancy. New York: Academic; 1979.

Beck DM, Schaefer C, Pang K, Carlson SM. Executive function in preschool children: Test-retest reliability. Journal of Cognition and Development. 2011; 12:169–193. [PubMed: 21643523]

Brown NC, Inder TE, Bear MJ, Hunt RW, Anderson PJ, Doyle LW. Neurobehavior at term and white and gray matter abnormalities in very preterm infants. The Journal of pediatrics. 2009; 155(1):32–38. [PubMed: 19394041]

Cao M, He Y, Dai Z, Liao X, Jeon T, Ouyang M, Huang H. Early development of functional network segregation revealed by connectomic analysis of the preterm human brain. Cerebral Cortex. 2016; 27(3):1949–1963.

Cao M, Huang H, He Y. Developmental connectomics from infancy through early childhood. Trends in Neurosciences. 2017; 40:494–506. [PubMed: 28684174]

Carlson SM, Zelazo PD. Minnesota Executive Function Scale: Test Manual. St. Paul, MH: Reflection Sciences; 2014.

Carpenter M, Nagell K, Tomasello M. Social cognition, joint attention, and communicative competence from 9 to 15 months of age. Monographs of the Society for Research in Child Development. 1998; 63:1–143.

Carter AS, Briggs-Gowan MJ, Jones SM, Little TD. The Infant–Toddler Social and Emotional Assessment (ITSEA): Factor Structure, Reliability, and Validity. Journal of Abnormal Child Psychology. 2003; 31:495–514. [PubMed: 14561058]

Carter AS, Volkmar FR, Sparrow SS, Wang JJ, Lord C, Dawson G, Fombonne E, Loveland K, Mesibov G, Schopler E. The vineland adaptive behavior scales: supplementary norms for individuals with autism. Journal of Autism and Developmental Disorders. 1998; 28:287–302. [PubMed: 9711485]

Chatham CH, Tayler KI, Charman T, Liogier D'ardhuy X, Eule E, Fedele A, Bolognani F. Adaptive behavior in autism: Minimal clinically important differences on the Vineland-II. Autism Research. 2017

Cholemkery H, Kitzerow J, Rohrmann S, Freitag CM. Validity of the social responsiveness scale to differentiate between autism spectrum disorders and disruptive behaviour disorders. European Child & Adolescent Psychiatry. 2014; 23:81–93. [PubMed: 23719758]

Chugani HT, Phelps ME. Maturational changes in cerebral function in infants determined by 18 FDG positron emission tomography. Science. 1986; 231:840–843. [PubMed: 3945811]

Chugani HT, Phelps ME, Mazziotta JC. Positron emission tomography study of human brain functional development. Annals of Neurology. 1987; 22:487–497. [PubMed: 3501693]

Constantino JN, Davis SA, Todd RD, Schindler MK, Gross MM, Brophy SL, Reich W. Validation of a breif quantitative measure of autistic traits: comparison of the social responsiveness scale with the autism diagnostic interview-revised. Journal of Autism and Developmental Disorders. 2003; 33:427–433. [PubMed: 12959421]

Constantino JN, Todd RD. Autistic Traits in the General Population: A Twin Stdy. Archives of General Psychiatry. 2003; 60:524–530. [PubMed: 12742874]

Courchesne E, Chisum HJ, Townsend J, Cowles A, Covington J, Egaas B, Press GA. Normal brain development and aging: quantitative analysis at in vivo MR imaging in healthy volunteers. Radiology. 2000; 216:672–682. [PubMed: 10966694]

Cox RW. AFNI: software for analysis and visualization of functional magnetic resonance neuroimages. Computers and Biomedical Research. 1996; 29:162–173. [PubMed: 8812068]

Croft S, Stride C, Maughan B, Rowe R. Validity of the Strengths and Difficulties Questionnaire in Preschool-Aged. Pediatrics. 2015; 135:e1210–e1219.https://doi.org/10.1542/peds.2014-2920 [PubMed: 25847804]

Csibra G, Davis G, Spratling MW, Johnson MH. Gamma oscillations and object processing in the infant brain. Science. 2000; 290:1582–1585. [PubMed: 11090357]

Damaraju E, Caprihan A, Lowe JR, Allen EA, Calhoun VD, Phillips JP. Functional connectivity in the developing brain: a longitudinal study from 4 to 9 months of age. Neuroimage. 2014; 84:169–180. [PubMed: 23994454]

Dean DC, Dirks H, O'Muircheartaigh J, Walker L, Jerskey BA, Lehman K, Deoni SCL. Pediatric neuroimaging using magnetic resonance imaging during non-sedated sleep. Pediatric Radiology. 2014; 44:64–72. [PubMed: 23917588]

Dehaene-Lambertz G, Spelke ES. The infancy of the human brain. Neuron. 2015; 88:93–109. [PubMed: 26447575]

Diamond A. Executive functions. Annual Review of Psychology. 2013; 64:135–168.

Doom J, Gunnar MR, Georgieff MK, Kroupina MG, Frenn K, Fuglestad AJ, Carlson SM. Beyond stimulus deprivation: Iron deficiency and cognitive deficits in post-institutionalized children. Child Development. 2014; 85:1805–1812. [PubMed: 24597672]

Dosenbach NU, Koller JM, Earl EA, Miranda-Dominguez O, Klein RL, Van AN, Wesevich V. Real-time motion analytics during brain MRI improve data quality and reduce costs. NeuroImage. 2017; 161:80–93. [PubMed: 28803940]

Dubois J, Poupon C, Thirion B, Simonnet H, Kulikova S, Leroy F, Dehaene-Lambertz G. Exploring the early organization and maturation of linguistic pathways in the human infant brain. Cerebral Cortex. 2016; 26:2283–2298. [PubMed: 25924951]

Eggebrecht AT, Elison JT, Feczko E, Todorov A, Wolff JJ, Kandala S, Pruett JR. Joint Attention and Brain Functional Connectivity in Infants and Toddlers. Cerebral Cortex. 2017; 27:1709–1720.https://doi.org/10.1093/cercor/bhw403 [PubMed: 28062515]

Emerson RW, Adams C, Nishino T, Hazlett HC, Wolff JJ, Zwaigenbaum L, Piven J. Functional neuroimaging of high-risk 6-month-old infants predicts a diagnosis of autism at 24 months of age. Science Translational Medicine. 2017; 9(393)

Emerson RW, Gao W, Lin W. Longitudinal study of the emerging functional connectivity asymmetry of primary language regions during infancy. Journal of Neuroscience. 2016; 36(42):10883–10892. [PubMed: 27798142]

Elison JT, Wolff JJ, Heimer DC, Paterson SJ, Gu H, Hazlett HC, Piven J. Frontolimbic neural circuitry at 6 months predicts individual differences in joint attention at 9 months. Developmental Science. 2013; 16:186–197.https://doi.org/10.1111/desc.12015 [PubMed: 23432829]

Evans AC. Brain Development Cooperative Group. The NIH MRI study of normal brain development. Neuroimage. 2006; 30:184–202. [PubMed: 16376577]

Fenson L, Marchman VA, Thal DJ, Dale PS, Reznick JS, Bates E. MacArthur-Bates Communicative Development Inventories. 2. Baltimore: Paul H. Brookes; 2007.

Fernandez-Miranda JC, Pathak S, Engh J, Jarbo K, Verstynen T, Yeh FC, Friedlander R. High-definition fiber tractography of the human brain: neuroanatomical validation and neurosurgical applications. Neurosurgery. 2012; 71:430–453. [PubMed: 22513841]

Fonov V, Evans AC, Botteron K, Almli CR, McKinstry RC, Collins DL. Brain Development Cooperative Group. Unbiased average age-appropriate atlases for pediatric studies. Neuroimage. 2011; 54:313–327. [PubMed: 20656036]

Fuglestad AJ, Whitley ML, Carlson SM, Boys CJ, Eckerle JK, Fink BA, Wozniak JR. Executive functioning deficits in preschool children with fetal alchohol spectrum disorders. Child Neuropsychology. 2015; 21:716–731. [PubMed: 25011516]

Gao W, Alcauter S, Elton A, Hernandez-Castillo CR, Smith JK, Ramirez J, Lin W. Functional network development during the first year: relative sequence and socioeconomic correlations. Cerebral Cortex. 2015; 25:2919–2928. [PubMed: 24812084]

Gao W, Lin W, Grewen K, Gilmore JH. Functional connectivity of the infant human brain: plastic and modifiable. Neuroscientist. 2016. https://doi.org/10.1177/1073858416635986

Gao W, Zhu H, Giovanello KS, Smith JK, Shen D, Gilmore JH, Lin W. Evidence on the emergence of the brain's default mode network from 2-week-old to 2-year-old healthy pediatric subjects. Proceedings of the National Academy of Sciences. 2009; 106:6790–6795.

Gartstein MA, Rothbrt MK. Studying infant temperament via the revised Infant Behavior Questionnaire. Infant Behavior & Development. 2003; 26:64–86.

Giedd JN, Blumenthal J, Jeffries NO, Castellanos FX, Liu H, Zijdenbos A, Rapoport JL. Brain development during childhood and adolescence: a longitudinal MRI study. Nature Neuroscience. 1999; 2:861–863. [PubMed: 10491603]

Gilmore JH, Shi F, Woolson SL, Knickmeyer RC, Short SJ, Lin W, Shen D. Longitudinal development of cortical and subcortical gray matter from birth to 2 years. Cerebral Cortex. 2012; 22:2478–2485. [PubMed: 22109543]

Gilmore JH, Zhai G, Wilber K, Smith JK, Lin W, Gerig G. 3 Tesla magnetic resonance imaging of the brain in newborns. Psychiatry Research: Neuroimaging. 2004; 132(1):81–85.

Glasser MF, Coalson TS, Robinson EC, Hacker CD, Harwell J, Yacoub E, Van Essen DC. A multi-modal parcellation of human cerebral cortex. Nature. 2016b; 536(7615):171–178.https://doi.org/10.1038/nature18933 [PubMed: 27437579]

Glasser MF, Smith SM, Marcus DS, Andersson JLR, Auerbach EJ, Behrens TEJ, Van Essen DC. The Human Connectome Project's neuroimaging approach. Nature Neuroscience. 2016a; 19(9):1175–1187.https://doi.org/10.1038/nn.4361 [PubMed: 27571196]

Gogtay N, Giedd JN, Lusk L, Hayashi KM, Greenstein D, Vaituzis AC, Thompson PM. Dynamic mapping of human cortical development during childhood through early adulthood. Proceedings of the National Academy of Sciences. 2004; 101:8174–8179.

Graham AM, Buss C, Rasmussen JM, Rudolph MD, Demeter DV, Gilmore JH, Fair DA. Implications of newborn amygdala connectivity for fear and cognitive development at 6-months-of-age. Developmental Cognitive Neuroscience. 2016; 18:12–25. [PubMed: 26499255]

Grayson DS, Fair DA. Development of large-scale functional networks from birth to adulthood: a guide to the neuroimaging literature. Neuroimage. 2017; 160:15–31. [PubMed: 28161313]

Hanson JL, Hair N, Shen DG, Shi F, Gilmore JH, Wolfe BL, Pollak SD. Family poverty affects the rate of human infant brain growth. PLoS ONE. 2013; 8:e80954. [PubMed: 24349025]

Hassinger-Das B, Jordan NC, Glutting J, Irwin C, Dyson N. Domain-general mediators of the relation between kindergarten number sense and first-grade mathematics achievement. Journal of Experimental Child Psychology. 2014; 118:78–92. [PubMed: 24237789]

Hazlett HC, Gu H, Munsell BC, Kim SH, Styner M, Wolff JJ, Piven J. Early brain development in infants at high risk for autism spectrum disorder. Nature. 2017; 542:348–351. [PubMed: 28202961]

Hazlett HC, Poe M, Gerig G, Smith RG, Provenzale J, Ross A, Gilmore J, Piven J. Magnetic resonance imaging and head circumference study of brain size in autism: birth through age 2 years. Archives of General Psychiatry. 2005; 62:1366–1376. [PubMed: 16330725]

Holland D, Chang L, Ernst TM, Curran M, Buchthal SD, Alicata D, Dale AM. Structural growth trajectories and rates of change in the first 3 months of infant brain development. JAMA Neurology. 2014; 71:1266–1274. [PubMed: 25111045]

Huang H, Shu N, Mishra V, Jeon T, Chalak L, Wang ZJ, He Y. Development of human brain structural networks through infancy and childhood. Cerebral Cortex. 2015; 25:1389–1404. [PubMed: 24335033]

Huppi PS. Cortical development in the fetus and the newborn: advanced MR techniques. Topics in Magnetic Resonance Imaging. 2011; 22:33–38. [PubMed: 22186904]

Huppi PS, Posse S, Lazeyras F, Burri R, Bossi E, Herschkowitz N. Magnetic resonance in preterm and term newborns: 1H-Spectroscopy in developing human brain. Pediatric Research. 1991; 30:574–578. [PubMed: 1666670]

Huppi PS, Warfiled S, Kikinis R, Barnes PD, Zientara GP, Jolesz FA, Volpe JJ. Quantitative magnetic resonance imaging of brain development in premature and mature newborns. Annals of Neurology. 1998; 43:224–235. [PubMed: 9485064]

Inder TE, Warfield SK, Wang H, Hüppi PS, Volpe JJ. Abnormal cerebral structure is present at term in premature infants. Pediatrics. 2005; 115(2):286–294. [PubMed: 15687434]

Jalbrzikowski M, Krasileva KE, Marvin S, Zinberg J, Andaya A, Bachman P, Bearden CE. Reciprocal social behavior in youths with psychotic illness and those at clinical high risk. Development and Psychopathology. 2013; 25:1187–1197. [PubMed: 24229557]

Jenkinson M, Beckmann CF, Behrens TEJ, Woolrich MW, Smith SM. FSL. Neuroimage. 2012; 62:782–790. [PubMed: 21979382]

Kidokoro H, Anderson PJ, Doyle LW, Woodward LJ, Neil JJ, Inder TE. Brain injury and altered brain growth in preterm infants: predictors and prognosis. Pediatrics. 2014 peds-2013.

Kim SH, Fonov VS, Dietrich C, Vachet C, Hazlett HC, Smith RG, Styner M. Adaptive prior probability and spatial temporal intensity change estimation for segmentation of the one-year-old human brain. Journal of Neuroscience Methods. 2013; 212:43–55. [PubMed: 23032117]

Knickmeyer RC, Gouttard S, Kang C, Evans D, Wilber K, Smith JK, Gilmore JH. A structural MRI study of human brain development from birth to 2 years. Journal of Neuroscience. 2008; 28:12176–12182. [PubMed: 19020011]

Kouider S, Stahlhut C, Gelskov SV, Barbosa LS, Dutat M, de Gardelle V, Christophe A, Dehaene S, Dehaene-Lambertz G. A neural marker of perceptual consciousness in infants. Science. 2013; 340:376–380. [PubMed: 23599498]

Kraemer HC, Yesavage JA, Taylor JL, Kupfer D. How can we learn about developmental processes from cross-sectional studies, or can we? American Journal of Psychiatry. 2000; 157:163–171. [PubMed: 10671382]

Kristen S, Sodian B, Thoermer C, Perst H. Infants joint attention skills predict toddlers' emerging mental state language. Developmental Psychology. 2011; 47:1207–1219. [PubMed: 21895365]

Kuhl PK, Tsao FM, Liu HH. Foreign-language experience in infancy: effects of short-term exposure and social interaction on phonetic learning. Proceedings of the National Academy of Sciences USA. 2003; 100:9096–9101.

Lebel C, Beaulieu C. Longitudinal development of human brain wiring continues from childhood into adulthood. Journal of Neuroscience. 2011; 31:10937–10947. [PubMed: 21795544]

Lee SJ, Steiner RJ, Yu Y, Short SJ, Neale MC, Styner MA, Zhu H, Gilmore JH. Common and heritable components of white matter microstructure predict cognitive function at 1 and 2 years. Proceedings of the National Academy of Sciences. 2016; 114:148–153.

Leppert IR, Almli CR, McKinstry RC, Mulkern RV, Pierpaoli C, Rivkin MJ, Pike GB. Brain Development Cooperative Group. T(2) relaxometry of normal pediatric brain development. Journal of Magnetic Resonance Imaging. 2009; 29:258–267. [PubMed: 19161173]

Lewis JD, Evans AC, Pruett JR, Botteron KN, McKinstry RC, Zwaigenbaum L, Piven J. The emergence of network inefficiencies in infants with autism spectrum disorder. Biological Psychiatry. 2017; 82:176–185. [PubMed: 28460842]

Lin W, Zhu Q, Gao W, Chen Y, Toh CH, Styner M, Gilmore JH. Functional connectivity MR imaging reveals cortical functional connectivity in the developing brain. American Journal of Neuroradiology. 2008; 29(10):1883–1889. [PubMed: 18784212]

Lyall AE, Shi F, Geng X, Woolson S, Li G, Wang L, Gilmore JH. Dynamic development of regional cortical thickness and surface area in early childhood. Cerebral Cortex. 2015; 25:2204–2212. [PubMed: 24591525]

Marrus N, Eggebrecht AT, Todorov A, Elison JT, Wolff JJ, Cole L, Pruett JR. Walking, gross motor development, and brain functional connectivity in infants and toddlers. Cerebral Cortex. 2017; 28(2):750–763.

Marrus N, Glowinski AL, Jacob T, Klin A, Jones W, Drain CE, Constantino JN. Rapid video-referenced ratings of reciprocal social behavior in toddlers: A twin study. Journal of Child Psychology and Psychiatry and Allied Disciplines. 2015; 56:1338–1346.https://doi.org/10.1111/jcpp.12391

Miller KL, Alfaro-Almagro F, Bangerter NK, Thomas DL, Yacoub E, Xu J, Smith SM. Multimodal population brain imaging in the UK Biobank prospective epidemiological study. Nature Neuroscience. 2016; 19:1523–1536. [PubMed: 27643430]

Mugler JP III, Bao S, Mulkern RV, Guttmann CR, Robertson RL, Jolesz FA, Brookeman JR. Optimized single-slab three-dimensional spin-echo MR imaging of the brain. Radiology. 2000; 216(3):891–899. [PubMed: 10966728]

Mukherjee P, Miller JH, Shimony JS, Conturo TE, Lee BCP, Almli CR, McKinstry RC. Normal brain maturation during childhood: developmental trends characterized with diffusion-tensor MR imaging. Radiology. 2001; 221:349–358. [PubMed: 11687675]

Mullen E. Mullen Scales of Early Learning. Circle Pines: American Guidance Service, Inc; 1995.

Mundy P, Newell L. Attention, joint attention, and social cognition. Current Directions in Psychological Science. 2007; 16:269–274. [PubMed: 19343102]

Neil JJ, Shiran SI, McKinstry RC, Schefft GL, Snyder AZ, Almli CR, Conturo TE. Normal brain in human newborns: apparent diffusion coefficient and diffusion anisotropy measured by using diffusion tensor MR imaging. Radiology. 1998; 209:57–66. [PubMed: 9769812]

Nelson PB, Adamson LB, Bakeman R. Toddlers' joint engagement experience facilitates preschoolers' acquisition of theory of mind. Developmental Science. 2008; 11:847–852. [PubMed: 19046153]

Nichols TE, Das S, Eickhoff SB, Evans AC, Glatard T, Hanke M, Yeo BTT. Best practices in data analysis and sharing in neuroimaging using MRI. Nature Neuroscience. 2016; 20:299–303.

Oguz I, Farzinfar M, Matsui J, Budin F, Liu Z, Gerig G, Styner M. DTIPrep: Quality control of diffusion-weighted images. Frontiers in Neuroinformatics. 2014; 8:4. [PubMed: 24523693]

Pascalis O, de Haan M, Nelson CA. Is face processing species-specific during the first year of life? Science. 2002; 296:1321–1323. [PubMed: 12016317]

Pelphrey KA, Reznick JS, Goldman BD, Sasson N, Morrow J, Donahoe A, Hodgson K. Development of visuospatial short-term memory in the second half of the 1st year. Developmental Psychology. 2004; 40:836–851. [PubMed: 15355170]

Pfefferbaum A, Mathalon DH, Sullivan EV, Rawles JM, Zipursky RB, Lim KO. A quantitative magnetic resonance imaging study of changes in brain morphology from infancy to late adulthood. Archives of Neurology. 1994; 51:874–887. [PubMed: 8080387]

Pine E, Luby J, Abbacchi A, Constantino JN. Quantitative assessment of autistic symptomatology in preschoolers. Autism. 2006; 10:344–352. [PubMed: 16908478]

Power JD, Barnes KA, Snyder AZ, Schlaggar BL, Petersen SE. Spurious but systematic correlations in fucntional connectivity MRI networks arise from subject motion. Neuroimage. 2012; 59:2142–2154. [PubMed: 22019881]

Power JD, Barnes KA, Snyder AZ, Schlaggar BL, Petersen SE. Steps toward optimizing motion artifact removal in functional connectivity MRI; a reply to Carp. Neuroimage. 2013; 76

Prager EO, Sera MD, Carlson SM. Executive function and magnitude skills in preschool children. Journal of Experimental Child Psychology. 2016; 147:126–139. [PubMed: 27082019]

Pruett JR, Kandala S, Hoertel S, Snyder AZ, Elison JT, Nishino T, Piven J. Accurate age classification of 6 and 12 month-old infants based on resting-state functional connectivity magnetic resonance imaging data. Developmental Cognitive Neuroscience. 2015; 12:123–133. [PubMed: 25704288]

Putnam SP, Gartstein MA, Rothbart MK. Measurement of fine-grained aspects of toddler temperament: The early childhood behavior questionnaire. Infant Behavior & Development. 2006; 29:386–401. [PubMed: 17138293]

Qiu A, Anh TT, Li Y, Chen H, Rifkin-Graboi A, Broekman BFP, Meaney MJ. Prenatal maternal depression alters amygdala functional connectivity in 6-month-old infants. Translational Psychiatry. 2015; 5:e508. [PubMed: 25689569]

Raudenbush SW. Comparing personal trajectories and drawing causal inferences from longitudinal data. Annual Review of Psychology. 2001; 52:501–525.

Remer J, Croeau-Chonka E, Dean DC, D'Arpino S, Dirks H, Whiley D, Deoni SCL. Quantifying cortial development in typically developing toddlers and young children, 1–6 years of age. Neuroimage. 2017; 153:246–261. [PubMed: 28392489]

Reznick JS, Morrow JD, Goldman BD, Snyder J. The onset of working memory in infants. Infancy. 2004; 6:145–154.

Scaife M, Bruner JS. The capacity for joint visual attention in the infant. Nature. 1975; 253:265–266. [PubMed: 1113842]

Shaw P, Greenstein D, Lerch J, Clasen L, Lenroot R, Gogtay N, Evans A, Rapoport J, Giedd J. Intellectual ability and cortical development in children and adolescents. Nature. 2006; 440:676–679. [PubMed: 16572172]

Shen MD, Kim SH, McKinstry RC, Gu H, Hazlett HC, Nordahl CW, Piven J. Increased extra-axial cerebrospinal fluid in high-risk infants who later develop autism. Biological Psychiatry. 2017; 82:186–193. [PubMed: 28392081]

Shi F, Yap PT, Wu G, Jia H, Gilmore JH, Lin W, Shen D. Infant brain atlases from neonates to 1- and 2-year-olds. PLoS One. 2011; 14:e18746.

Short SJ, Elison JT, Goldman BD, Styner M, Gu H, Connelly M, Gilmore JH. Associations between white matter microstructure and infants' working memory. NeuroImage. 2013; 64:156–166.https://doi.org/10.1016/j.neuroimage.2012.09.021 [PubMed: 22989623]

Smith SM, Jenkinson M, Woolrich MW, Beckmann CF, Behrens TE, Johansen-Berg H, Matthews PM. Advances in functional and structural MR image analysis and implementation as FSL. Neuroimage. 2004; 23(Suppl 1):S208–S219. [PubMed: 15501092]

Smyser CD, Inder TE, Shimony JS, Hill JE, Degnan AJ, Snyder AZ, Neil JJ. Longitudinal analysis of neural network development in preterm infants. Cerebral Cortex. 2010; 20:2852–2862. [PubMed: 20237243]

Sparrow SS, Cicchetti DV, Balla DA. Vineland-II adaptive behavior scales, second edition, survey forms manual. Bloomington, MN: PsychCorp; 2005.

Swanson MR, Wolff JJ, Elison JT, Gu H, Hazlett HC, Botteron K, Piven J. Splenium development and early spoken language in human infants. Developmental Science. 2015; 20https://doi.org/10.1111/desc.12360

Tahiroglu D, Moses LJ, Carlson SM, Mahy CE, Olofson EL, Sabbagh MA. The children's social understanding scale: Construction and validation of a parent-report measure for assessing individual differences in children's theory of mind. Developmental Psychology. 2014; 50:2485–2497. [PubMed: 25264702]

Tavor I, Jones OP, Mars RB, Smith SM, Behrens TE, Jbabdi S. Task-free MRI predicts individual differences in brain activity during task performance. Science. 2016; 352(6282):216–220. [PubMed: 27124457]

Tomasello M, Carpenter M, Call J, Behne T, Moll H. Understanding and sharing intentions: the origins of cultural cognition. Behavioral and Brain Sciences. 2005; 28:675–735. [PubMed: 16262930]

Toulmin H, Beckmann CF, O'Muircheartaigh J, Ball G, Nongena P, Makropoulos A, Edwards AD. Specialization and integration of functional thalamocortical connectivity in the human infant. Proceedings of the National Academy of Sciences. 2015; 112:6485–6490.

Tustison NJ, Avants BB, Cook PA, Zheng Y, Egan A, Yushkevich PA, Gee JC. N4ITK: improved N3 bias correction. IEEE Transactions in Medical Imaging. 2010; 29:1310–1320.

Ugurbil K, Xu J, Auerbach EJ, Moeller S, Vu AT, Duarte-Carvajalino JM, Yacoub E. Pushing spatial and temporal resolution for functional and diffusion MRI in the Human Connectome Project. Neuroimage. 2013; 80:80–104. [PubMed: 23702417]

van den Heuvel MP, Kersbergen KJ, de Reus MA, Keunen K, Kahn RS, Groenendaal F, Benders MJ. The neonatal connectome during preterm brain development. Cerebral cortex. 2014; 25(9):3000–3013. [PubMed: 24833018]

Van Essen DC, Smith SM, Barch DM, Behrens TEJ, Yacoub E, Ugurbil K. WU-Minn HCP Consortium. The WU-Minn Human Connectome Project : An overview. NeuroImage. 2013; 80:62–79.https://doi.org/10.1016/j.neuroimage.2013.05.041 [PubMed: 23684880]

Veraart J, Poot DH, Van Hecke W, Blockx I, Van der Linden A, Verhoye M, Sijbers J. More accurate estimation of diffusion tensor parameters using diffusion kurtosis imaging. Magnetic resonance in medicine. 2011; 65(1):138–145. [PubMed: 20878760]

Wan MW, Brooks A, Green J, Abel K, Elmadih A. Psychometric and validation of a brief rating measure of parent-infant interaction: Manchester assessment of caregiver-infant interaction. International Journal of Behavioral Development. 2017; 41:542–549.

Wang J, Vachet C, Rumple A, Gouttard S, Ouziel C, Perrot E, Styner M. Multi-atlas segmentation of subcortical brain structures via the AutoSeg software pipeline. Fronteirs in Neuroinformatics. 2014; 8:7.

Wang L, Gao Y, Shi F, Li G, Gilmore JH, Lin W, Shen D. LINKS: Learning-based multi-source IntegratioN frameworK for Segmentation of infant brain images. NeuroImage. 2015; 108:160–172.http://doi.org/10.1016/j.neuroimage.2014.12.042 [PubMed: 25541188]

Willett JB, Singer JD, Martin NC. The design and analysis of longitudinal studies of development and psychopathology in context: statistical models and methodological recommendations. Development and Psychopathology. 1998; 10:395–426. [PubMed: 9635230]

Wolff JJ, Swanson MR, Elison JT, Gerig G, Pruett JR, Styner MA, Piven J. Neural circuitry at age 6 months associated with later repetitive behavior and sensory responsiveness in autism. Molecular Autism. 2017; 8:8. [PubMed: 28316772]

Yap PT, Chen Y, An H, Yang Y, Gilmore JH, Lin W, Shen D. SPHERE: SPerical Harmonic Elastic REgeistration of HARDI data. Neuroimage. 2011; 55:545–556. [PubMed: 21147231]

Yap PT, Shen D. Spatial transformation of DWI data using non-negative sparse representation. IEEE Transactions on Medical Imaging. 2012; 31:2035–2049. [PubMed: 22711770]

Yap PT, Zhang Y, Shen D. Multi-tissue decomposition of diffusion MRI signals via L0 sparse-group estimation. IEEE Transactions on Image Processing. 2016; 25:4340–4353. [PubMed: 27392357]

Zhang H, Schneider T, Wheeler-Kingshott CA, Alexander DC. NODDI: practical in vivo neurite orientation dispersion and density imaging of the human brain. Neuroimage. 2012; 61:1000–1016. [PubMed: 22484410]

Zhang W, Li R, Deng H, Wang L, Lin W, Ji S, Shen D. Deep convolutional neural networks for multi-modality isointense infant brain image segmentation. Neuroimage. 2015; 108:214–224. [PubMed: 25562829]

Zhang Y, Shi F, Wu G, Wang L, Yap PT, Shen D. Consistent spatial-temporal longitudinal atlas construction for developing infant brains. IEEE Transactions of Medical Imaging. 2016; 35:2568–2577.

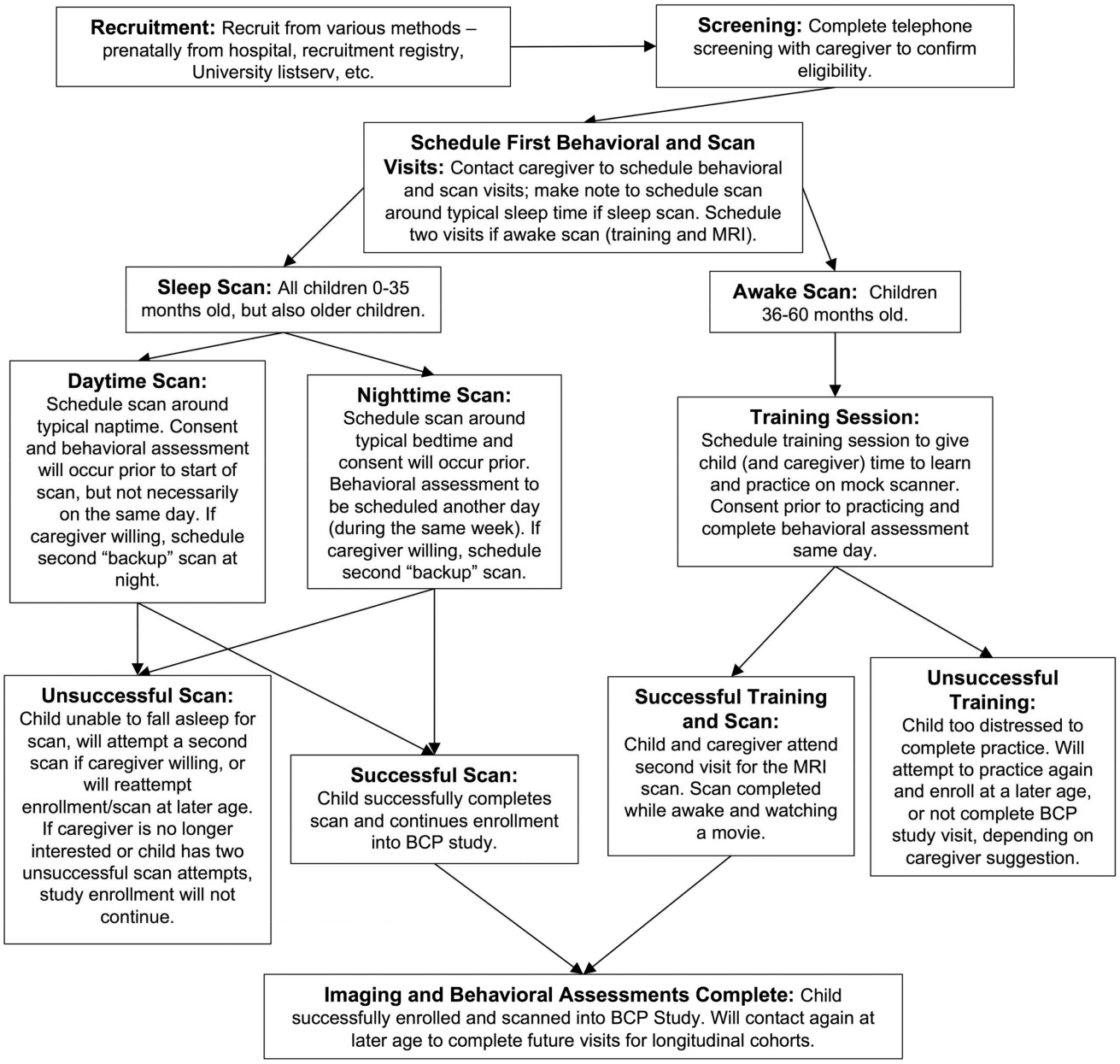

Figure 1.
Subject flow for the Baby Connectome Project

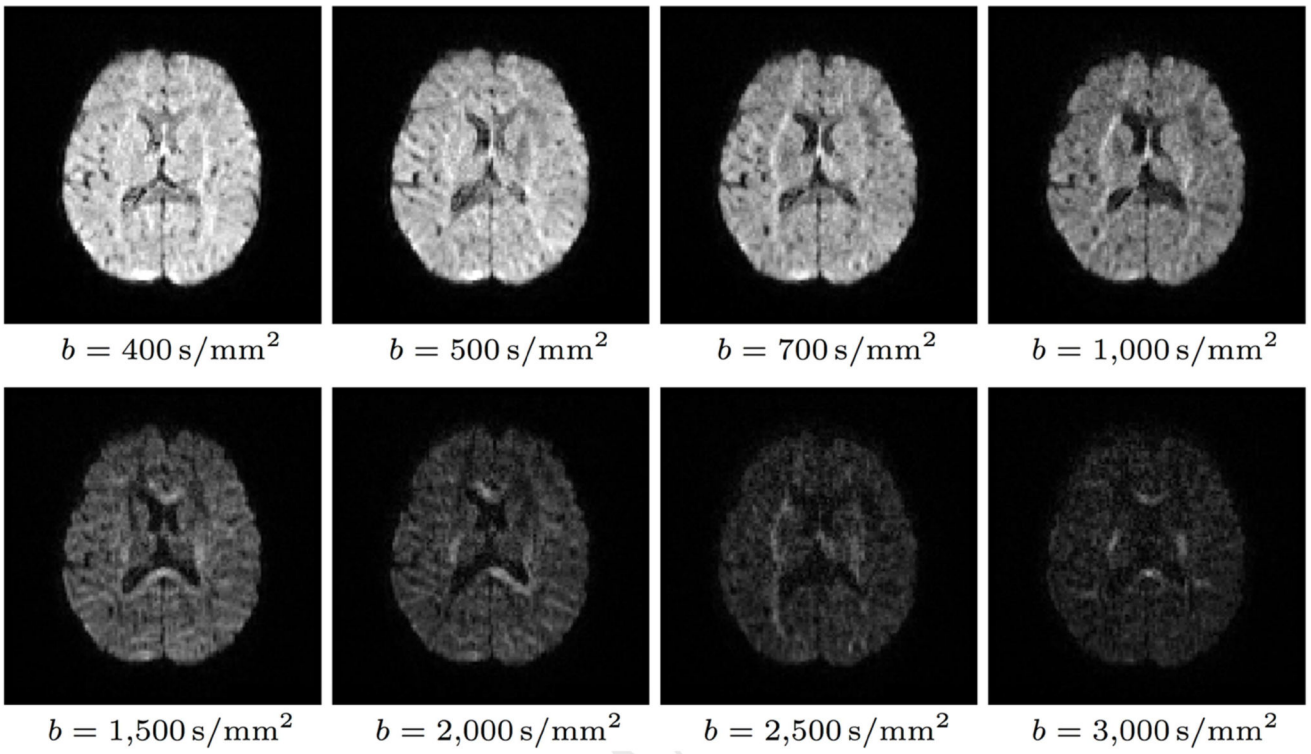

Figure 2.
Diffusion-weighted images for different *b*-values in a representative 6-month-old dataset.

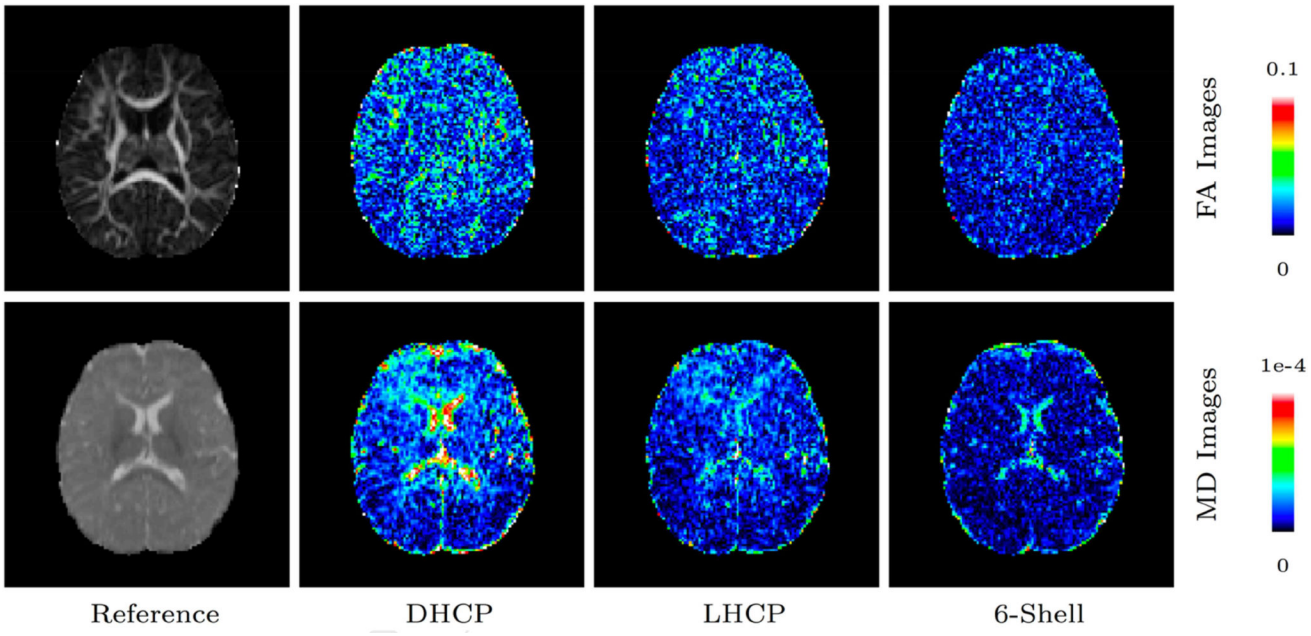

Figure 3.
FA and MD absolute difference maps of a 6-month-old for the different sampling schemes in comparison with the reference dataset.

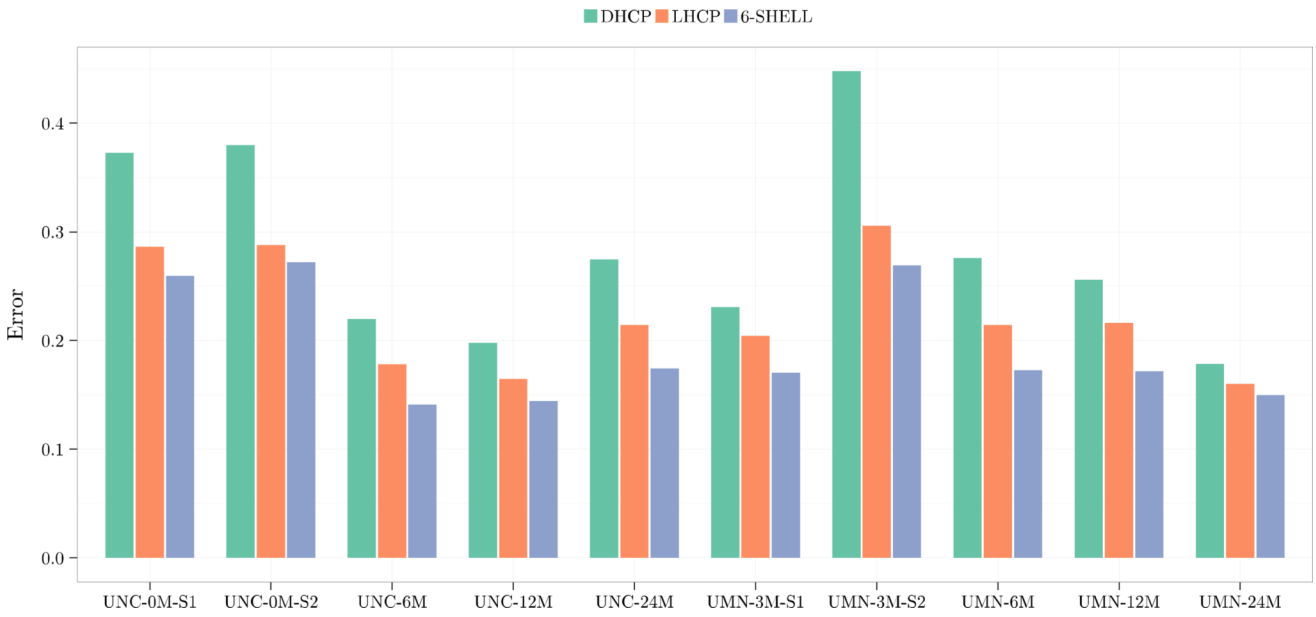

Figure 4.
FA normalized absolute differences.

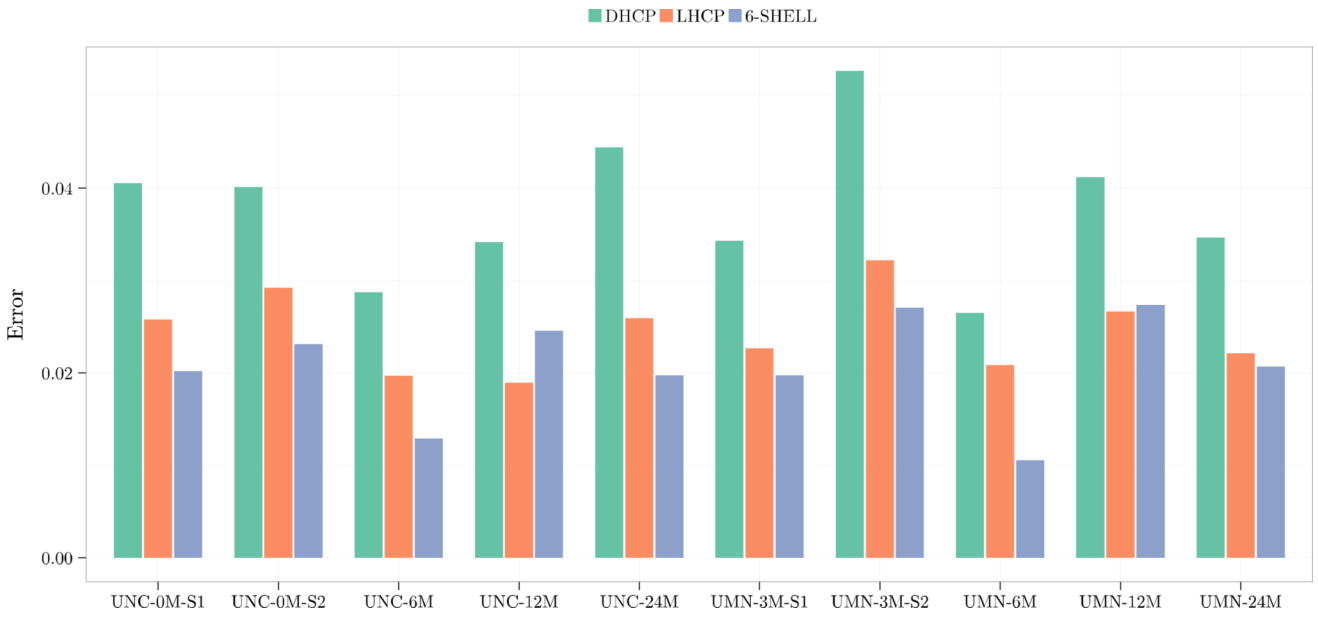

Figure 5.
MD normalized absolute differences.

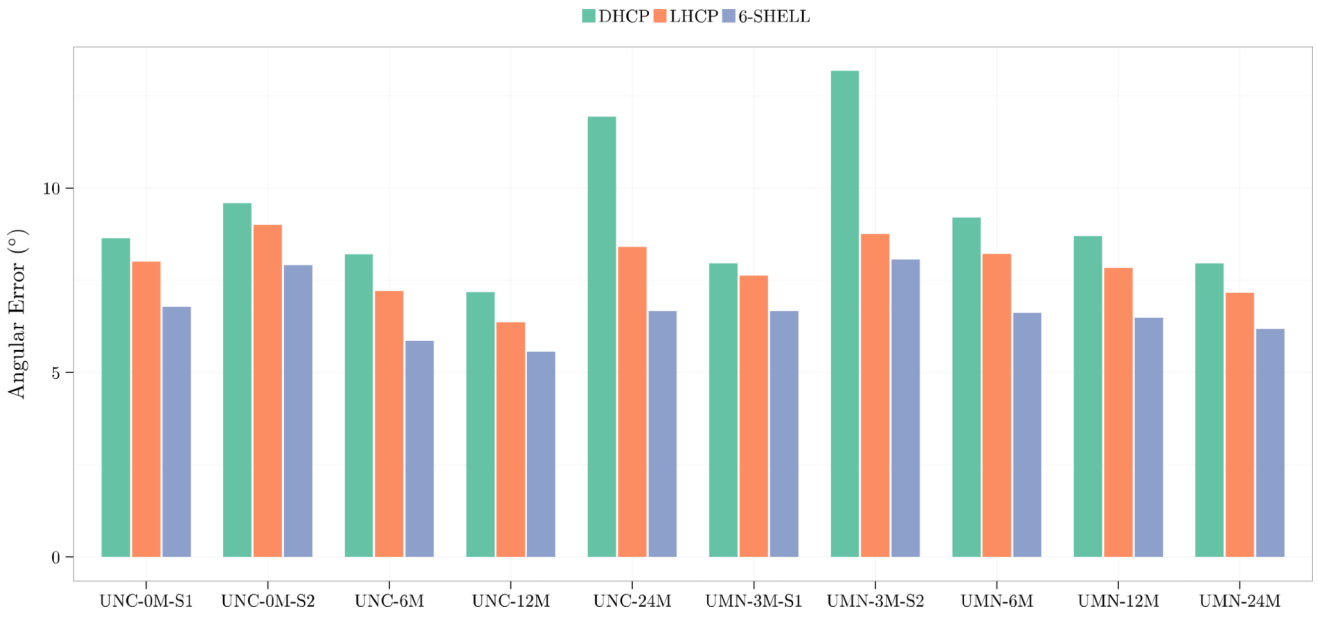

Figure 6.
Angular accuracy of fiber orientations estimated using the tensor model.

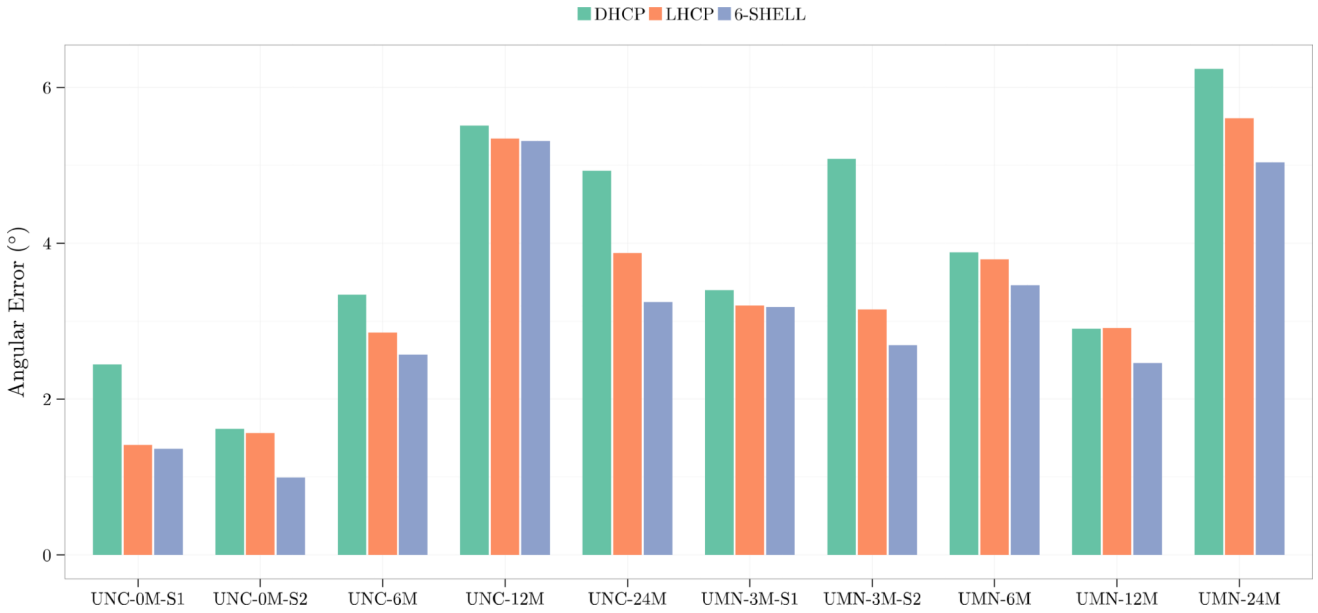

Figure 7.
Angular accuracy of fiber orientations estimated using the multi-tissue model.

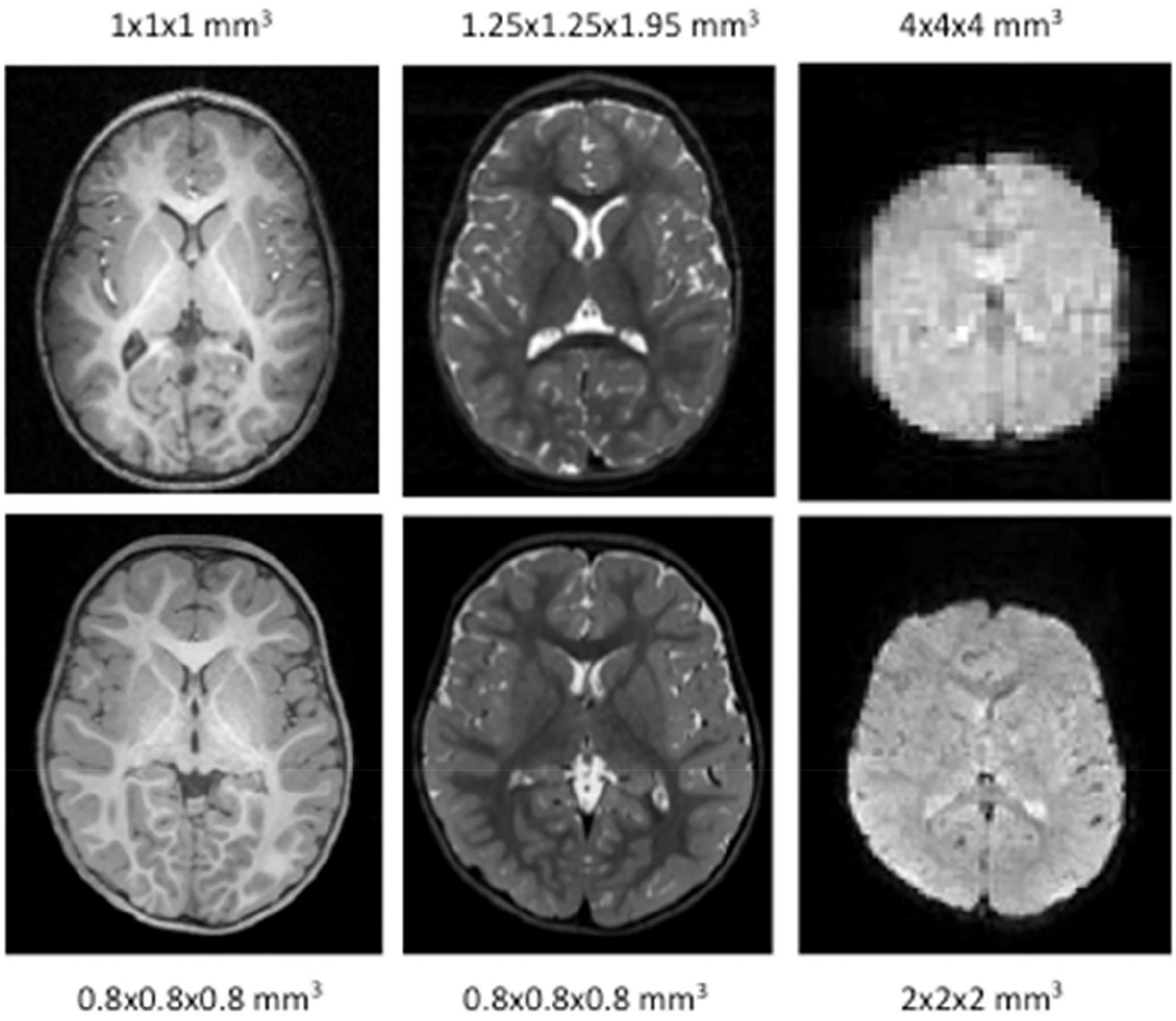

Figure 8.
T1w, T2w, and resting BOLD quality from two 24-month-olds

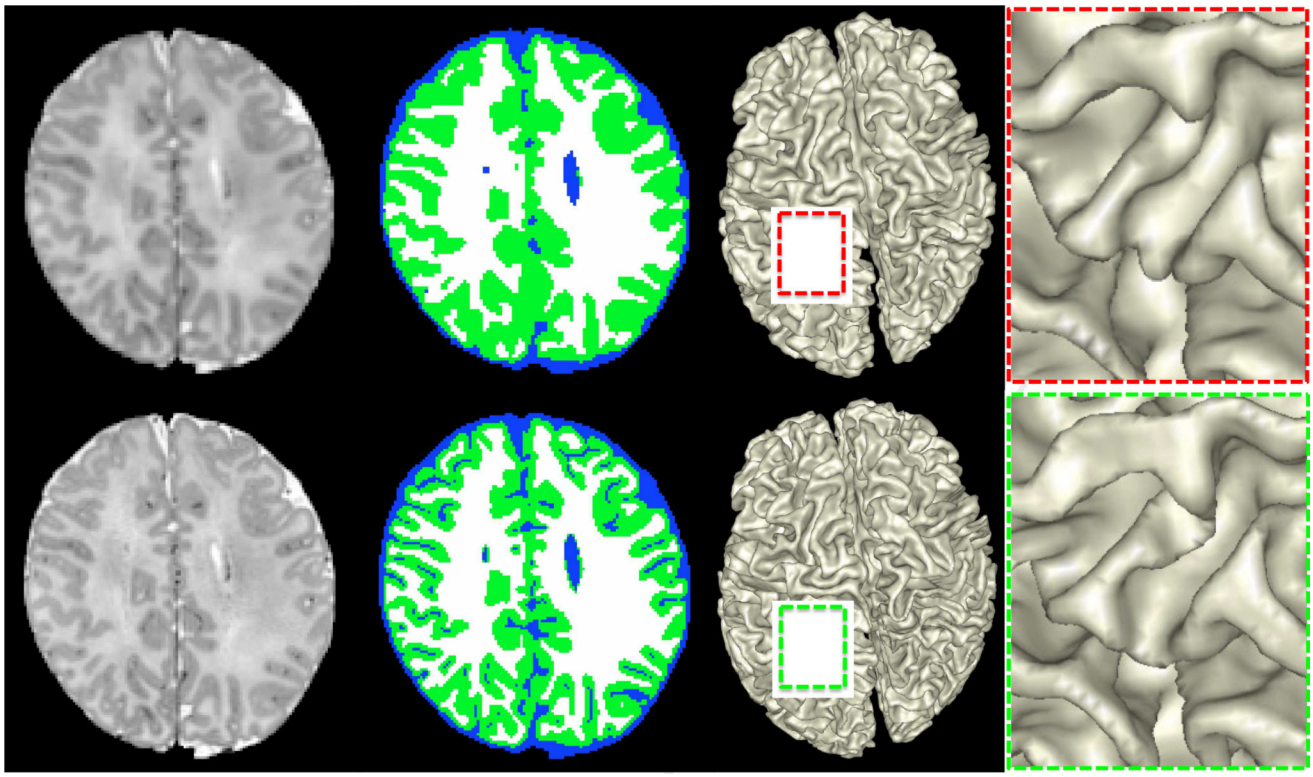

Figure 9.

The upper and lower rows show the comparison results on the same neonatal subject (scanned 18 days after birth) with different spatial resolutions: $1mm^3$ and $0.5mm^3$. From left to right: intensity image, segmentation, WM/GM rendering, and zoomed views for better visualization.

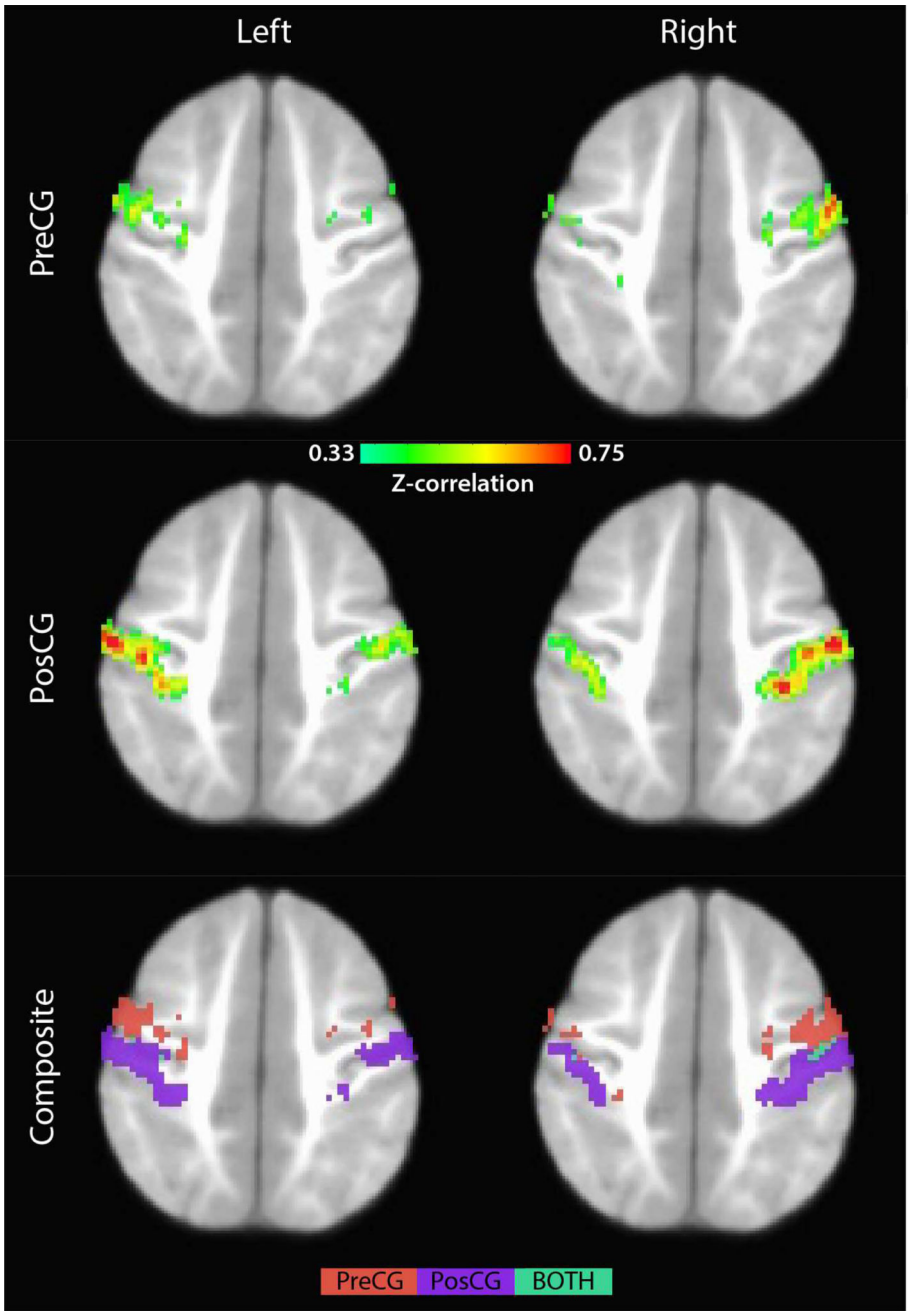

Figure 10.
Intrinsic functional connectivity networks for seeds placed in the pre- and post-central gyrus.

Table 1

Longitudinal Sampling Plan, total n = 285.

		Age at Assessment (m = months)						
Cohort	**# of subjects**	**Visit 1**	**Visit 2**	**Visit 3**	**Visit 4**	**Visit 5**	**Visit 6**	**Total Visits**
A1	15	Birth-2 wk	3m	6m	9m	12m	**24m**	6
A2	15	1m	4m	7m	10m	13m	**24m**	6
A3	15	2m	5m	8m	11m	14m	**24m**	6
B1	20	9m	12m	15m	18m	21m	24m	6
B2	20	10m	13m	16m	19m	22m	25m	6
B3	20	11m	14m	17m	20m	23m	26m	6
C1	20	15m	21m	27m	33m			4
C2	20	16m	22m	28m	34m			4
C3	20	17m	23m	29m	35m			4
D1	20	18m	24m	**30m**	36m			5
D2	20	19m	25m	**31m**	37m			5
D3	20	20m	26m	**32m**	38m			5
E1 *	15	3m	6m	9m	12m			5
E2 *	15	4m	7m	10m	13m			5
E3 *	15	5m	8m	11m	14m			5
E4 *	15	6m	9m	12m	15m			5

Cohorts E1–E4 noted with a * come from R01 MH104324 (PI J. Elison). Bolded cells indicate behavioral data collection only.

Table 2

BCP Neuroimaging Protocol.

	Matrix	FOV (mm)	Resolution (mm)	Flip Angle	TE (msec)	TR (msec)	Slices Orientation	AF/ MB	Time (min:sec)
Localizer			0.5×0.5×0.7	20	5	30			0:43
MPRAGE	320×320	256×256	0.8×0.8×0.8	8	2.24	2400/1060	208/Sag	AF=2	6:38
T2wSPC	320×320	256×256	0.8×0.8×0.8	VAR	564	3200	208/Sag	AF=2	5:57
Field_Map-PA	104×91	208×208	2×2×2	90	66	8000	72/Axial	MB=1	0:33
Field_Map-AP	104×91	208×208	2×2×2	90	66	8000	72/Axial	MB=1	0:33
Resting BOLD-PA	104×91	208×208	2×2×2	52	37	800	72/Axial	MB=8	5:47
Resting BOLD-AP	104×91	208×208	2×2×2	52	37	800	72/Axial	MB=8	5:47
DWI-PA (6 shell)	140×105	210×210	1.5×1.5×1.5	78 excite/160 refocus	88.6	2640	95/Axial	MB=5	6:58
DWI-AP (6 shell)	140×105	210×210	1.5×1.5×1.5	78 excite/160 refocus	88.6	2640	95/Axial		6:58
	Contingent on the baby continuing to sleep								
Resting BOLD-PA	104×91	208×208	2×2×2	52	37	800	72/Axial	MB=8	5:47
Resting BOLD-AP	104×91	208×208	2×2×2	52	37	800	72/Axial	MB=8	5:47
DWI-PA (2 shell)	140×105	210×210	1.5×1.5×1.5	78 excite/160 refocus	89.2	3222	92/Axial	MB=4	4:35
DWI-AP (2 shell)	140×105	210×210	1.5×1.5×1.5	78 excite 160 refocus	89.2	3222	92/Axial	MB=4	4:35

Table 3

Sampling schemes for dMRI optimization pilot test.

Protocol Name	b-values (s/mm^2)	# gradient directions	# of b_0 scans	# DW images
DHCP	400, 1000, 2600	32,44,64	10	140
LHCP	700, 1500, 3000	36,48,60	10	144
6-shell	500, 1000, 1500, 2000, 2500, 3000	9,12,17,24,34,48	6	144

Note that the number of gradient directions correspond to the b values in the order they appear.